UNC-5134
Volume I

CFSTI PRICES

H.C. $ 4.00 ; MN 75

CARBIDE FUEL DEVELOPMENT

FINAL REPORT
PERIOD OF MAY 15, 1959 TO OCTOBER 15, 1965

A. Strasser
D. Stahl

October 15, 1965

Work Performed under UNC Project 2320
Contract AT(30-1)-2899 and Project IV,
Contract AT(30-1)-2303 with the
United States Atomic Energy Commission

Prime Contractor
UNITED NUCLEAR CORPORATION
Research and Engineering Center
Elmsford, New York

Subcontractor
THE CARBORUNDUM COMPANY
Niagara Falls, New York

Work Performed by

United Nuclear Corporation

N. Chu
R. Jaroszeski
G. Sofer
D. Stahl
A. Strasser
O. Sullivan

The Carborundum Company

J. Andersen
C. McMurtry
K. Taylor

DISCLAIMER

FOREWORD

The Carbide Fuel Development Program was sponsored by the USAEC, Division of Reactor Development. The United Nuclear Corporation performed conceptual design, fuel evaluation, and fuel irradiation. Under its prime contract with the AEC, the United Nuclear Corporation, Development Division, issued a subcontract to The Carborundum Company for fuel fabrication.

The authors wish to thank the many people whose talents and diligent work contributed to this program.

TABLE OF CONTENTS

TABLES

FIGURES

1. INTRODUCTION

The Carbide Fuel Development Program was concerned with the technology of the entire UC-PuC fuel cycle. The major goals of the program were to produce (UPu)C* and to obtain data on its irradiation behavior for long burnups and at high power generation rates. In addition, other areas of the fuel cycle were explored to discover possible problems. The program was initiated in May 1959 and was completed in October 1965.

Fuel made of a combination of UC and PuC has a potential of reducing the fuel cycle cost of existing fast breeder reactors. This is because of the increased burnup and increased power generation capability of (UPu)C compared to presently available metallic fuels. Irradiation tests to 38×10^{20} fiss/cm^3 (113,000 Mwd/T) indeed show that (UPu)C is structurally stable and releases less fission gas than oxide fuel irradiated at comparable power. Because of the high melting and good thermal conductivity of (UPu)C, the fuel is capable of high power generation rates.

This is the final report on the project.

Volume I of this report summarizes previously reported work on the conceptual fuel element design, fuel fabrication, and out-of-pile property measurements.

*(UPu)C indicates a solid solution of UC and PuC.

Volume II summarizes all of the irradiation data previously reported up to 13×10^{20} fiss/cm^3 (40,000 Mwd/T) and now brought up to date to 38×10^{20} fiss/cm^3 (114,000 Mwd/T). The previously reported data can be found in greater detail in the respective progress reports (listed in the bibliography). The new data on the highest burnup irradiation tests are presented here in detail.

All of the work under this contract investigated mixed carbides at 20 w/o PuC level with the exception of the property measurements, which were made on 5 w/o PuC fuel. A closely allied project under AEC Contract AT(30-1)-3118 investigated the properties of fuel at the 20 w/o PuC level.*

*Stahl, D., Strasser, A.: Out-of-Pile Properties of Mixed Uranium-Plutonium Carbides, UNC-5074 (Dec. 1963).

2. SUMMARY AND CONCLUSIONS

2.1 ANALYTICAL STUDY

Heat transfer, nuclear and preliminary cost studies were conducted to evaluate the potential of carbide fuels in fast breeder power reactors. In these analytical studies, carbide fuel elements were substituted in the core of the Enrico Fermi Fast Breeder Reactor (EFFBR) and their effect on the reactor heat transfer characteristics, nuclear characteristics, and fuel cycle cost was calculated and compared to U-10% Mo and PuO_2-UO_2 fuels. A summary of the results is given in Table 2.1.

The calculations indicated that carbide fuels offer the promise of significant reduction in the fuel cycle cost of fast breeder power reactors by virtue of: (1) their favorable heat transfer characteristics, i.e., high thermal conductivity and high melting point, and (2) their high burnup potential.

Larger fuel rod diameters and a smaller number of rods per core are possible with carbide than with U-10% Mo or $(UPu)O_2$.

The breeding ratio of (UPu)C is greater than that of oxide and metallic uranium but less than metallic plutonium fuel. The critical mass required is greater than for oxides and less than for metallic fuel.

The fuel cost of the EFFBR with a (UPu)C core is expected to be lower than with U-10% Mo, even if burnup were unchanged. This is primarily the result of savings

TABLE 2.1 — SUMMARY OF ANALYTICAL STUDY RESULTS

Reactor	A Reference EFFBR U-10% Mo Core	B EFFBR UC Core			C EFFBR (UPu)C Core		D EFFBR $(UPu)O_2$ Core
Heat Transfer Characteristics							
Number of fuel pins per subassembly	144		36			36	225
Fuel pin diameter, in.	0.148		0.289			0.289	0.104
Corresponding maximum fuel temperature, °F	1135		2900			2900	3900
Nuclear Characteristics							
Calculated breeding ratio	1.12		1.09			1.57	1.48
Critical mass, kg U^{235} or Pu^{239}	433		397			279	253
Estimated Fuel Costs							
Fuel fabrication cost, $/kg (U+Pu)	540	←	340*	→	←	550*	→ 2200*
Assumed burnup, a/o of (U+Pu)	1.25	1.25	2.0	5.0	2.0	5.0	2.0
Fuel cost, mills/kwh (Pu at $30/g)	8.8	7.3	4.7	2.1	6.4	2.9	18.1
Fuel cost, mills/kwh (Pu at $12/g)	11.7	10.0	7.4	4.9	5.9	3.4	16.4

*Based on pressing, sintering, and grinding pellets. Relaxation of tolerances to eliminate grinding will reduce fuel cycle costs more on Pu cores than others.

realized in the fuel fabrication steps, reflecting the larger fuel pin diameter of (UPu)C. With the higher burnup possible with carbides, the fuel cost goes down to a fraction of the cost with U-10% Mo. Reduction in the number and complexity of fabrication operations, such as elimination of pellet grinding, will result in cost reductions. Fuel costs are expected to be much higher for $(UPu)O_2$ fuel than for (UPu)C mainly because of the large number of small pins needed to satisfy the heat transfer requirements. The fabrication cost estimate for $(UPu)O_2$ fuel was based on pelletizing and grinding.

2.2 FUEL FABRICATION

A process with economical mass production potential was developed to produce high density (UPu)C pellets. The starting materials, UO_2, PuO_2, and C were blended and reacted at 1625°C to produce a (UPu)C clinker. The clinker was crushed to a fine powder, cold pressed, and sintered at 1525°C to 95% minimum theoretical density with 0.1 w/o nickel sintering aid, or sintered at 1925°C to 91 w/o theoretical density without sintering aid. The process was used to prepare samples for out-of-pile and in-pile property measurements at 5 w/o and 20 w/o PuC levels.

Several other processes using oxides as starting materials were investigated, but they were found to be less economical.

Prior to experiments with solid solution uranium-plutonium carbides, essentially stoichiometric UC powder was prepared by the carbon reduction of UO_2 in a helium atmosphere. Attempts to prepare stoichiometric PuC by the carbon reduction of PuO_2 failed (the product consisted of a mixture of plutonium carbides and oxides). Pu_2C_3 and $(UPu)_2C_3$ was readily obtained by reacting stoichiometric amounts of PuO_2, UO_2, and C.

2.3 FUEL PROPERTIES

2.3.1 Structural Characterization

Sintering $(U_{0.8}Pu_{0.2})C$ at 1500°C with 0.1 w/o Ni sintering aid produced a structure of monocarbide with a second phase of sesquicarbide. Sintering without sintering aid at 1900°C or higher produced monocarbide with a second phase of dicarbide.

The plutonium and nickel were distributed homogeneously within the sensitivity of a microprobe analyzer.

High temperature heat treatment (1750 to 2200°C) in vacuum caused the nickel to diffuse to the grain boundaries. In vacuum, the nickel could be evaporated. Some of the residual oxygen in pellets could be reacted by vacuum heat treatment and removed as CO, with an attendant slight swelling and decrease in density.

The lattice parameter of $(U_{0.8}Pu_{0.2})C$ did not change significantly in seven months.

2.3.2 Fuel-Clad Compatibility

Tests up to 820°C for 4000 hr show that UC is compatible with type 304 stainless steel, 2¼ Cr-1 Mo steel, and pure Nb. The tests show that UC reacted with Inconel-X, beryllium, and Zircaloy-2.

$(U_{0.95}Pu_{0.05})C$ was compatible with type 316 stainless steel, 2¼ Cr-1 Mo steel, pure Nb and Nb-1 w/o Zr alloy. It reacted with Zircaloy-2.

2.3.3 Coefficient of Expansion

The coefficient of expansion of $(U_{0.95}Pu_{0.05})C_{0.98}$ at 25 to 1400°C was measured as 12.6×10^{-6}/°C, and that of $(U_{0.95}Pu_{0.05})C_{0.98}$ + 1 w/o Ni at 25 to 1400°C was measured as 12.2×10^{-6}/°C. The expansion curves were smooth and indicated that no transformations occurred.

2.3.4 Melting Point

The melting (liquidus) temperature of $(U_{0.95}Pu_{0.05})C_{0.98}$ was determined to be 2535 ± 20°C. The solidus temperature was estimated to be 2500 ± 20°C.

2.3.5 Vapor Pressure

The vapor pressures of uranium and plutonium over $(U_{0.95}Pu_{0.05})C_{0.98}$ were measured by the Knudsen effusion technique. They were:

°C	Uranium, atm	Plutonium, atm
1822	9×10^{-8}	1 to 2×10^{-6}
1995	0.3×10^{-6}	1 to 2×10^{-5}

The plutonium vaporized at a higher rate than the uranium. The uranium vapor pressure over (UPu)C was similar to that of uranium over UC. The difficulty in maintaining constant sample composition at high temperatures for relatively long times increased the difficulty of the measurements.

2.4 FUEL IRRADIATION

Irradiation tests of 12 clad $(U_{0.8}Pu_{0.2})C$ specimens in the range of 7×10^{20} fiss/cm^3 (20,000 Mwd/T) to 38×10^{20} fiss/cm^3 (113,000 Mwd/T) at 490 to 570 w/cm (avg) demonstrated the excellent structural and dimensional stability of the fuel. The microstructure of the fuel was essentially unchanged by irradiation. The fuel OD increased 0.5 to 0.6% per a/o burnup. The fission gas release increased significantly from less than 1% at 7×10^{20} fiss/cm^3 and 1% at 13×10^{20} fiss/cm^3 to 30% at 38×10^{20} fiss/cm^3. This was accompanied by a significant increase in fuel porosity at the center. No significant differences were noted between the 91% dense fuel without sintering aid, and the 95% dense fuel made with 0.1 w/o Ni sintering aid.

The irradiation tests demonstrated the good thermodynamic compatibility of helium bonded (UPu)C with stainless steel up to 9200 hr at fast breeder reactor operating conditions, and with niobium well beyond those conditions.

The six niobium-clad specimens were sound and in excellent condition. The clad OD was unchanged up to 11×10^{20} fiss/cm^3 (35,000 Mwd/T). At 36×10^{20} fiss/cm^3 (114,000 Mwd/T), there was an average 2.5% OD increase. Of the six stainless steel-clad specimens, one was in excellent condition, one failed because of an experiment malfunction, and four were ruptured as a result of the drastic decrease in steel ductility to a level below that required to accommodate strains from fuel expansion and thermal stresses.

The brittle stainless steel ruptures point to the major problem to be solved for carbide fuel elements, as well as for other ceramic fuels, i.e., the accommodation of fuel swelling at high burnups without disruption of the clad. Even the small diametral increases of 0.6% per a/o burnup amount to a sufficiently large change at 10 a/o burnup to put the already weakened clad under a severe strain.

Prior to the (UPu)C irradiations, two capsules containing three clad UC specimens were irradiated to a maximum burnup of 6.2×10^{20} fiss/cm^3 (18,600 Mwd/T). The primary function of the irradiation was to test the capsule design, methods of fuel center temperature measurement, and in-pile fission gas pressure measurement.

The results of the test indicated that the capsule design was reliable, and that fuel center temperature measurement was practical. The design of the in-pile fission gas pressure measurement probe proved too risky, without further development, for plutonium specimens.

3. ANALYTICAL STUDY*

3.1 INTRODUCTION

In order to evaluate the future potential of carbide fuels for fast breeder power reactors, the characteristics of several carbide-fueled reactors of this type were investigated. Heat transfer, nuclear, and cost studies were performed for both uranium carbide (UC) and uranium-plutonium carbide combinations (UPu)C. In these studies, carbide fuel elements were substituted for the presently planned fuels in the current designs of several fast reactors. Over-all reactor performance and design characteristics, such as power output, core size, coolant temperatures, and coolant flow rate were kept constant, so that a direct comparison could be made of the effects of fuel substitution. The number and size of fuel element subassemblies were also kept constant to obtain a design which would permit testing of individual carbide fuel subassemblies in the parent reactor. Since this approach imposes some restrictions on the utilization of carbide fuels, the benefits obtained are expected to fall short of the maximum benefits possible with design optimizations based on carbide fuels alone.

Heat transfer calculations were performed for the Enrico Fermi Fast Breeder Reactor (EFFBR) and the Experimental Breeder Reactors (EBR-I and II). The number of fuel pins required per subassembly, and the corresponding pin diameter were determined as a function of maximum fuel temperature. Nuclear calculations of critical mass, enrichment, and breeding ratio were performed for

*Completed in October 1959. Reported in References 1 and 7.

the EFFBR. Order of magnitude fuel cost studies were made comparing carbide fuel at several burnups to the reference U-10% Mo EFFBR and a hypothetical EFFBR fueled with combined uranium-plutonium oxide. The EFFBR was selected for the nuclear and cost calculations because more data are available on fuel costs for this reactor than for the EBR's.

3.2 DESIGN STUDIES

3.2.1 Heat Transfer Studies

A. Effect of Heat Transfer on Configuration

The number of fuel rods needed to deliver a given amount of power depends upon the physical properties of the fuel elements as well as the design characteristics of the reactor. In this study, carbide fuel elements were substituted in several present reactor designs, using the same fuel subassembly external dimensions and the same coolant flow area per subassembly as in the reference reactor. The number of carbide elements required is a function primarily of the maximum allowable carbide temperature. The high melting point (~2500°C), high permissible operating temperature (~1000°C min), and good thermal conductivity of uranium carbide suggest the possibility of using fewer – and larger – rods than in the reference metallic uranium designs.

The results of the heat transfer analysis are summarized in Table 3.1. An increase in the maximum fuel temperature permits a greater temperature drop across the fuel pin. Because the heat generated per unit length of fuel rod is directly proportional to the temperature drop across the fuel and is independent of the rod diameter, the number of rods required to produce a given power will decrease as the maximum fuel temperature is allowed to increase. The pin diameters given in Table 3.1 were chosen to yield the same flow area, and, therefore, the same coolant temperatures and flow velocity as the reference reactors. Standard heat transfer equations were used in the analysis.

TABLE 3.1 — RESULTS OF THE HEAT TRANSFER STUDY

	EFFBR					
	U-10% Mo	UC or (UPu)C				$(UPu)O_2$
Maximum fuel temp, °C	610	910	1030	1600	2010	2150
Thermal bond	Metallurgical bond	10 mils NaK	←	0.5 mil He	→	1.0 mil He
Fuel thermal conductivity, Btu/hr-°F-ft*	~16.2	12.1	12.1	12.1	12.1	1.0
Number of fuel rods per subassembly	144	81	81	36	25	225
Fuel rod diameter, in.	0.148	0.172	0.190	0.289	0.348	0.104
Clad thickness†	0.050 (Zr)	0.010	0.010	0.013	0.015	0.010

	EBR-II					EBR-I	
	U-Fissium	UC or (UPu)C				U-2% Zr	UC or (UPu)C
Maximum fuel temp, °C	640	870	980	1320	1880	390	930
Thermal bond	6 mils NaK	10 mils NaK	←	0.5 mil He	→	Metallurgical bond	1 mil He
Fuel thermal conductivity, Btu/hr-°F-ft*	~17	12.1	12.1	12.1	12.1	~15.1	12.1
Number of fuel rods per subassembly	91	61	61	37	19	36	6
Fuel rod diameter, in.	0.144	0.173	0.191	0.249	0.355	0.364	0.853
Clad thickness, in.	0.009	0.009	0.010	0.011	0.015	0.020 (Zr)	0.037

*The out-of-pile UC thermal conductivity at 1400°F was used for the UC and (UPu)C rods. The best estimate for UO_2 thermal conductivity at high temperatures was used for $(UPu)O_2$ rods.

†Clad material is stainless steel except when noted.

Because of the lack of experience with carbide fuels at the time the study was made, the maximum permissible fuel temperature was uncertain. Therefore, several maximum fuel temperatures were assumed and the corresponding number of fuel rods per subassembly and fuel rod diameter were calculated. The results have been shown in Table 3.1.

While the present EFFBR subassembly design uses 144 metallic uranium fuel rods, the most conservative carbide design, in which the maximum carbide temperature is under 1090°C (2000°F), requires only 81 rods. A design allowing a 1590°C (2900°F) maximum carbide temperature further reduces the required number of rods to 36. Finally, at a maximum temperature of 2010°C (3650°F), which is well below the carbide melting point, only 25 carbide rods are needed. In contrast to the uranium carbide elements, 225 rods per subassembly would be required with $(UPu)O_2$ fuel for a maximum temperature of 2150°C (3900°F). The greatly increased number of rods is due to the lower thermal conductivity of $(UPu)O_2$.

The present EBR-II design uses 91 metallic uranium fuel rods. Carbide designs with maximum temperatures of 980°C (1800°F), 1320°C (2400°F), and 1880°C (3400°F) would require 61, 37, and 19 rods, respectively.

The results of heat transfer calculations for the EBR-I indicate that six uranium carbide fuel rods, with a maximum temperature of 930°C (1700°F), may be substituted for the 36 metallic uranium rods in each fuel subassembly. Since the EBR-I is a relatively low specific power, low temperature reactor, there is less incentive to utilize the high specific power, high temperature potential of carbide fuel in this reactor.

The thermal conductivities of the fuels were not well-known at the time the study was made. Therefore, the following assumptions were made:

1. The thermal conductivity of UC was assumed to be constant up to 1980°C (3600°F) since the values known at the time which extended up to 760°C (1400°F) varied only slightly with the temperature.

2. The thermal conductivity of (UPu)C was assumed to be the same as UC.

3. The thermal conductivity of $(UPu)O_2$ was assumed to be the same as UO_2.

B. Effect of Fuel-to-Clad Gap

A 0.5-mil radial helium gap between the carbide and inner clad surface was assumed in obtaining the above heat transfer results. A larger gap would result in an excessive temperature drop across the helium, which would reduce the efficient utilization of the high fuel temperature. A smaller gap is impractical. The temperature drop across the cladding and the coolant film is comparatively small and its influence is therefore subordinated to that of the helium gap.

Several approaches can be taken to design the fuel-to-clad gap. Initial ceramic fuel element designs, such as PWR UO_2 rods, considered the relative expansion of fuel and cladding. By specifying very close dimensional tolerances on the OD of the fuel (±0.0005 in. for PWR) and ID of the cladding, the fuel and cladding were designed to just touch at operating conditions. The fuel rods designed on this principle performed well, but were expensive to fabricate.

Irradiation experience on UO_2 with less stringent dimensional tolerances has served as the basis for a less conservative approach in the design of the fuel-to-clad gap. Runnalls[16] and Robertson have reported that the surface temperature of UO_2 starting with a 0.017-in. diametral, cold, fuel-clad gap did not rise during irradiation more than 100°C (210°F) over that of UO_2 starting with a 0.005-in. diametral, cold, fuel-clad gap. Tests were with 0.67-in. diameter pellets clad in Zircaloy-2; center temperatures were near the melting point. The explanation proposed was that cracked segments of oxide shift radially outward and contact

the cladding. The fuel-to-clad temperature drop then becomes a function of contact pressure and the surface condition of fuel and cladding. Ability of fuel to relocate itself from an unfavorable heat transfer position to a more favorable one has been noted by Bates and Roake.[17] They irradiated UO_2 powder packed to 4 g/cm^3 in Zircaloy-2, at heat fluxes as high as 700,000 Btu/hr/ft^2 at central melting temperatures. The fuel sintered to at least 9.3 g/cm^3 during irradiation, and the shrinkage was taken axially. The dense UO_2 filled the cladding radially. UC may behave in the same manner as UO_2. The decreased allowable tolerances would decrease the fuel cycle costs below the estimates made in Section 3.3.

An additional method of circumventing the problem of strict tolerance is the use of a low melting point metal bond between the fuel and cladding. Sodium or NaK are used, but they pose compatibility problems between fuel and stainless steel. The experience with low melting point metal bonds and ceramic fuels operating above the boiling points of the bond material is limited. The ceramic fuels will crack, and the bond material could become heated above its boiling point.

The substitution of a 10-mil NaK bond (radial gap) for the helium in the low temperature UC designs of the EFFBR and EBR-II would reduce the maximum carbide temperature from 1030°C and 980°C to 910°C and 870°C respectively (see Table 3.1). The advantages gained did not seem to justify the attendant liquid-metal bond development problems in the initial development of (UPu)C, and it was decided to design and test helium-filled fuel rods.

3.2.2 Nuclear Studies

A. Comparison of Carbide with Uranium Alloy and Oxide Designs

The nuclear characteristics of the EFFBR were estimated by one-dimensional, 10-group, diffusion-theory calculations. The purpose of these calculations was to uncover significant differences between metallic, carbide, and oxide fuels, rather

than to determine accurate absolute values of critical mass and breeding ratio. A one-dimensional spherical model was used, and suitable correction factors were applied to allow for deviation from the actual EFFBR geometry.

In this study all reactors were calculated cold, clean, and with control rods withdrawn. The critical mass was adjusted to yield an excess reactivity of approximately one dollar. The important parameters calculated were critical mass, enrichment, and breeding ratio. The significant results of the nuclear analysis are presented in Table 3.2, following a listing of the physical characteristics of the designs in question.

Reactor A represents the reference EFFBR design. The core of this reactor is fueled with a U-10% Mo alloy encased in a Zircaloy-2 clad. The calculated critical mass of 433 kg is in fair agreement with 444 kg reported by APDA.[18] A breeding ratio of 1.12* was calculated compared with 1.20 reported by APDA.[18]† The breeding ratio expected in the EFFBR appears to be uncertain, as a value of 1.12 was reported in another publication.[19] Breeding ratios are given in Table 3.2 as determined from the 10-group calculations, and also normalized to a breeding ratio of 1.20 for the reference EFFBR.

Reactor B represents an EFFBR which contains UC fuel. Because the blanket rods of the reference EFFBR are relatively large and their burnup at discharge is well below the metallurgical limit, carbide blanket elements do not offer any significant advantage. The use of carbide elements in the blanket might result in a decrease of the U^{238} captures because of the lower uranium density. Therefore, the reference reactor blanket design was maintained in all reactors considered.

---

*Defined at U^{238} captures per U^{235} core absorption.

†The reported APDA critical mass and breeding ratio may be based, at least in part, on past calculations performed by UNC for APDA. However, these UNC calculations were made using a multigroup code different from the one used in the present work.

TABLE 3.2 — REACTOR CHARACTERISTICS

Reactor	A Reference EFFBR U-10% Mo Core	B EFFBR UC Core	C EFFBR (UPu)C Core	D EFFBR $(UPu)O_2$ Core
Physical Characteristics				
Core				
Power, Mw	265	265	265	265
Volume, ft^3	11.65	11.65	11.65	11.65
Fuel material diam, in.	0.148	0.289	0.289	0.104
Cladding material	Zr	SS	SS	SS
Cladding thickness, in.	0.005	0.013	0.013	0.010
No. of pins per subassembly	144	36	36	225
No. of fuel subassemblies	91	91	91	91
Volume fractions, %				
Fuel material	33.7	33.1	33.1	27.3
Cladding	4.9	5.5	5.5	11.3
Coolant	47.2	47.2	47.2	47.2
Subassembly walls	14.2	14.2	14.2	14.2
Blanket				
Power, Mw	35	35	35	35
Volume, ft^3	174	174	174	174
Fuel material	U-2.75% Mo	U-2.75% Mo	U-2.75% Mo	U-2.75% Mo
Fuel material diam, in.	0.415	0.415	0.415	0.415
Cladding material	SS	SS	SS	SS
Cladding thickness in.	0.010	0.010	0.010	0.010
Nuclear Characteristics				
k_{eff}	1.008	1.008	1.006	1.005
Critical mass, kg U^{235} or Pu^{239}	433	397	279	253
Enrichment, %				
Core	25.0	27.9	19.4	28.1
Blanket	0.35	0.35	0.35	0.35
Breeding ratio				
Core	0.32	0.28	0.48	0.30
Blanket	0.80	0.81	1.09	1.18
Total	1.12	1.09	1.57	1.48
Total, normalized to 1.2 for reactor A	1.20	1.17	1.68	1.59

The important changes caused by the fuel substitution in the core are: (1) introduction of carbon in the fuel, (2) removal of molybdenum alloying material, and (3) a necessary increase in enrichment (ratio of U^{235}/U^{238}) resulting from the lower density of the carbide fuel. These changes tend to increase reactivity and thereby reduce the critical mass.

The slowing down characteristics of the carbon result in an increase in reactivity by shifting the neutron energy spectrum to regions of higher importance. Molybdenum acts primarily as a neutron absorber and its removal tends to improve neutron economy and increase reactivity. Finally, U^{238} in the core also acts as neutron absorber, capturing more neutrons than it produces by fast fissions. Hence its removal causes an increase in reactivity. The net result is that the calculated critical mass in the uranium carbide reactor is 397 kg, or about 8% less than in the reference reactor. Because of the lower uranium content in the carbide reactor, an increase in enrichment from 25.0 to 27.9% is required.

The effect of replacing the fuel of EFFBR with uranium carbide is not beneficial in all respects, as it leads to a somewhat lower breeding ratio. The breeding ratio of reactor B was calculated as 1.09, which is about 3% less than the breeding ratio of the reference design. This decrease is due to a 13% decrease in the core breeding ratio. The blanket breeding ratio remains essentially unchanged.

The next reactor examined was an EFFBR with (UPu)C core (reactor C). The uranium in the core is depleted uranium from diffusion plant tailings containing 0.37% U^{235}. The calculated Pu^{239} critical mass, 279 kg, is 30% smaller than the U^{235} critical mass of reactor B. The reduced critical mass is characteristic of plutonium-fueled reactors, and is caused primarily by the higher value of ν for plutonium. The breeding ratio was calculated as 1.57, which is approximately 40% greater than the UC and the reference reactors.

The next reactor was an EFFBR fueled with a $(UPu)O_2$ mixture (reactor D). Because of the small rod diameter required, the volume fraction of cladding is a factor of two larger than in reactor C, leaving a smaller volume for the oxide fuel. In addition, the density of U (or Pu) in mixed oxide is about 20% less than the density of U (or Pu) in the combined carbide. Therefore, the total number of heavy atoms (U + Pu) in reactor D is 38% less than in reactor C. This leads to a substantially higher plutonium enrichment for reactor D than in reactor C, i.e., a substantial reduction of the U^{238}/Pu^{239} ratio. This removal of U^{238} from the core tends to increase the reactivity of the core, resulting in a lower critical mass. The critical mass calculated for the PuO_2 reactor is 253 kg of Pu^{239} which is 9% less than the corresponding critical mass for the PuC reactor. The breeding ratio of reactor D is 1.48 or 6% lower than that for the PuC reactor.

B. Compensation for Reactivity Loss at High Burnup

One of the important advantages of carbide fuels is their high burnup potential. Whereas metallic uranium alloys are limited in burnup, the burnup limit of carbide might be factors of 3 or 4 times as great.

The length of time that individual fuel subassemblies are allowed to remain in the reactor core is determined by the metallurgical fission damage the fuel elements can withstand. The small excess reactivity available to compensate for fuel element burnup and growth shortens the time between successive refueling shutdowns compared to the allowable fuel residence time, even for U-10% Mo fuel. In order to compensate for reactivity losses, partial reloadings are employed so that individual subassemblies may be irradiated to their maximum metallurgical burnup. In the reference EFFBR partial reloadings are planned at biweekly intervals. The number of fuel subassemblies which are withdrawn at each shutdown is 16 out of 91 core subassemblies for $1\frac{1}{4}\%$ burnup. As the metallurgical burnup is increased, the number of fuel subassemblies withdrawn may be proportionately decreased.

To compensate for large losses in reactivity resulting from fission product build-up and fuel growth, additional U^{235} or Pu may be added to the core. It was estimated[8] by APDA that an increase in core loading of 1.65% over the clean cold value for each 1¼% burnup would be required for the U-10% Mo-fueled reactor. It should be noted that this increase in core loading cannot be introduced at start-up, but must be achieved gradually as the average core burnup increases, by adding additional subassemblies at the edge of the core. A similar increase in the core loading would be required in the carbide-fueled reactors.

C. Temperature Coefficients of Reactivity

An estimate of the magnitude of the coefficients of reactivity was made for the UC-fueled EFFBR. This estimate was based on extrapolations from values reported for the reference EFFBR. The various effects are discussed below.

Axial Fuel Expansion

The effect of axial fuel expansion is to reduce fuel density. This has a negative effect on reactivity. It is partially offset by the increase in the length of the core which would tend to reduce leakage. The net effect is negative for the U-10% Mo and is given[18] as -2.8×10^{6} $\Delta k/k/°C$. Since the linear expansion coefficient for UC is about 11.6×10^{-6} in./in.-°C compared with 18×10^{-6} in./in.-°C for U-10% Mo fuel, it might be expected that the net effect of axial fuel expansion for the UC carbide designs would be negative but smaller in magnitude than the U-10% Mo figure.

Ejection of Coolant by Fuel Radial Expansion

Since the danger coefficient of sodium is positive throughout the core (Fig. 30 of Reference 18), the expulsion of sodium due to radial expansion of fuel should have a negative effect on reactivity. The temperature coefficient of reactivity for this effect is given[18] as -0.5×10^{-6} $\Delta k/k/°C$ for U-10% Mo fuel. Again, because of the

smaller linear expansion coefficient of the carbide fuel, it might be expected that this effect for UC would be negative but smaller in magnitude.

Reduced Sodium Density

Heating of the sodium results in reduced sodium density and, as in the radial expansion of the fuel, the effect on reactivity is negative. In a UC-fueled EFFBR this effect should also be negative and of about the same order of magnitude as for U-10% Mo fuel which is given[18] as -3.0×10^{-6} $\Delta k/k/°C$.

Radial Expansion of the Core

The radial expansion of the core results from the expansion of stainless steel fuel subassembly walls which are made to touch each other by pads provided to prevent bowing of individual subassemblies. The corresponding coefficient of reactivity is expected to be negative and of nearly the same magnitude as the U-10% Mo fuel, which is given[18] as -3.0×10^{-6} in./in.-°C.

Doppler Broadening

An increase in core temperature results in broadening of resonances of U^{238} captures (negative effect on reactivity) and U^{235} fissions (positive effect). These effects counterbalance each other at approximately 50% enrichment. For U-10% Mo, the effect is given[18] as -1.6×10^{-6} $\Delta k/k/°C$. Since a somewhat higher enrichment is used with UC fuel, the effect is somewhat smaller in magnitude, but again it is negative.

The net result of the above considerations is that all temperature coefficients for UC fuel are negative though the over-all temperature coefficient of reactivity is smaller in magnitude than for U-10% Mo fuel. Best estimates for UC fuel are given in Table 3.3.

TABLE 3.3 — ISOTHERMAL CORE TEMPERATURE COEFFICIENTS OF REACTIVITY

	$\Delta k/k/°C, \times 10^{-6}$	
	U-10% Mo (Reference 18)	UC
Axial Fuel Expansion	-2.8	~-1.6
Ejection of Sodium	-0.5	~-0.3
Reduced Sodium Density	-6.1	~-6.0
Radial Expansion of Core	-3.0	~-3.0
Doppler Effect Total Core	-1.6	~-1.5
Total Core	-14.0	~-12.0

All temperature coefficients for the PuC-fueled reactor are also negative. However, the magnitude of individual coefficients could not be directly estimated from the data on the reference EFFBR.

3.3 COST STUDIES

The results of the heat transfer and nuclear studies were used to estimate and compare fuel cycle costs for the EFFBR fueled with metallic, carbide, and oxide fuels. The physical and nuclear characteristics of the reactors considered in the cost comparison are given in Table 3.2. Breeding ratios normalized to 1.2 for the reference reactor were used in the calculations.

One of the most important factors affecting nuclear fuel costs is the allowable burnup of the fuel material. A 1¼% burnup corresponding to the presently anticipated value for the EFFBR was assumed for the reference reactor.* Several burnups ranging from 1¼ to 5% were considered in the cost estimate of the UC reactor. The cost calculations were patterned after the method outlined by the Edison Electric Institute,[20] and the results of the calculations are given in terms of quantities defined in Reference 20.

Because of the many uncertainties connected with nuclear fuel costs, the reliability of the comparison will depend on the assumptions made. The important fuel cost assumptions used in this study are presented in Table 3.4. Perhaps both the most important and the most uncertain cost is the fuel fabrication cost. The fabrication costs, given in Table 3.4, include the cost of conversion of UF_6 to fuel material, fabrication of fuel material into the finished fuel element, and inspection of the final fuel elements. Fabrication costs for the reference U-10% Mo reactor were calculated from data published by APDA in Reference 21. Carbide fabrication costs were obtained partly from The Carborundum Company and partly by extrapolation from data available for UO_2, corrected for the size, number, and

*Burnup defined as the atom per cent of the heavy isotopes (U+Pu) fissioned. In U-10% Mo, 1.26% uranium burnup corresponds to 1% alloy burnup.

TABLE 3.4 — FUEL COST ASSUMPTIONS FOR EFFBR

	Core A (U-10% Mo)	Core B (UC)	Core C (UPu)C	Core D $(UPu)O_2$	Blanket
Fuel Fabrication Cost, C_f, $/kg (U+Pu)					
UF_6 to fuel material	145	110	12	5	11
Pu nitrate to fuel material	–	–	145	141	–
Powder to pellets (excluding losses)	–	11	33	38	–
Fabrication (including labor assembly, inspection, cladding material)	304	123	243	1853	51
Losses during fabrication and pelletizing, assumed at 2% (Pu at $30/g)	87	91	118	172	–
Shipping fresh fuel	2	2	2	2	2
Total	538	337	553	2211	64

Fuel Material Losses, %	
Conversion UF_6 to fuel material	1.5
Pelletizing	2.0
Reprocessing	1.5
Plutonium recovery	1.0
Fuel Cycle Working Capital Charges, %/yr*	12
Fuel Material Lease Charge, %/yr	4
Plant Factor, %	80
Plant Efficiency, %	33
Reprocessing Charges, $/day for a 1000-kg U/day capacity plant	15,300

*Applied to fuel fabrication cost of one reactor loading, and value of purchased depleted uranium.

enrichment of the fuel rods. The carbide fabrication method assumed was preparation of carbide powder by the oxide-carbon reaction and pressing-sintering the powder into pellets. Allowance was made for higher conversion cost from UF_6 to UC than UF_6 to UO_2. The lower fabrication cost of UC elements compared to the reference is primarily due to the fewer number of fuel rods required.

Because of its high alpha activity and toxicity, handling and fabrication of plutonium is expected to be more expensive than corresponding operations with uranium. Therefore, although the number and size of fuel elements are the same for the UC and PuC-fueled reactors, fabrication costs for PuC will be higher. Because of the relatively large number of rods required, fabrication cost for the PuO_2-fueled reactor is expected to be very high.

The results of the cost studies are presented in Table 3.5. By virtue of a smaller fabrication cost, the UC reactor, even at 1¼% burnup, has a lower fuel cost than the reference reactor. At 2% burnup, which should easily be achieved with carbide fuels, the fuel cycle cost of the uranium carbide-fueled reactor is approximately one-half of the corresponding reference cost, and at 5% burnup the UC cost is less than one-fourth the reference cost.

Although at corresponding burnups a larger net fuel material credit is obtained in the PuC reactor, increased fabrication costs and lease charges cause a slightly higher total fuel cycle cost than that obtained with the corresponding UC reactor. The cost is, however, still considerably less than the reference reactor. The extremely high fabrication costs cause the fuel costs of the PuO_2 design to be more than twice that of the reference.

Fuel cycle costs using $12/g as the value of plutonium are also given in Table 3.5.

TABLE 3.5 — TOTAL FUEL CYCLE COSTS FOR EFFBR, MILLS/KWH(e)*

	Reactor A	Reactor B-1	Reactor B-2	Reactor B-3	Reactor C	Reactor C	Reactor D
Material	U-10% Mo	UC	UC	UC	(UPu)C	(UPu)C	$(UPu)O_2$
Burnup	1¼%	1¼%	2%	5%	2%	5%	2%
Fissionable Material Destroyed or Lost, M_U†	3.36	3.49	2.99	2.53	4.84	4.32	5.57
Credit for Pu Formed, M_{Pu}	-4.73	-4.57	-4.57	-4.56	-6.55	-6.55	-6.28
Net Fuel Material Cost, M_m	-1.37	-1.08	-1.58	-2.03	-1.71	-2.23	-0.71
Fuel Fabrication Cost, M_f‡	6.19	4.25	3.04	1.82	4.33	2.34	14.26
Spent Fuel Processing Cost, M_p	1.37	1.40	1.16	0.98	1.27	1.08	1.24
Fuel Cycle Working Capital Cost, M_c	0.63	0.55	0.55	0.55	0.61	0.61	0.81
Fuel Material Lease Cost, M_ℓ	2.00	2.15	1.50	0.82	1.90	1.05	2.50
Total Fuel Cost, M_t (Pu at $30/g)	8.82	7.27	4.70	2.14	6.40	2.85	18.10
Total Fuel Cost (Pu at $12/g)	11.66	10.02	7.44	4.88	5.85	3.38	16.41

*Reactors B, C, and D not optimized for respective fuels. For reactor descriptions see Table 3.2.

†Symbols correspond to definitions given by the Edison Institute.[20]

‡Based on pressing, sintering, and grinding pellets. Relaxation of tolerances to eliminate grinding would reduce costs more on Pu cores than others. See Table 3.4 for additional details.

4. FUEL FABRICATION*

4.1 INTRODUCTION

The goal of the fabrication studies was to produce high density solid solution (UPu)C pellets by fabrication techniques which have a potential for economic mass production. Fuel of high physical density (about 95% of theoretical) was desired which minimizes fission gas release, gives a high fuel density, and has a high thermal conductivity.

The two major carbide preparation routes are the carbothermic reduction of fuel oxides and the reaction of metallic fuel with carbon or hydrocarbon gas. Oxide was chosen as a starting material instead of metal, because fuel recycling produces oxide several steps before it could produce metal. Particularly for a remote operation the cost of oxide would be considerably less than metal.

The three major carbide powder consolidation processes are cold pressing and sintering, vibratory compaction, and arc casting. The cold pressing and sintering process was chosen for this study because it was a simple, well-developed method and because the advantages outweighed the disadvantages when compared to arc casting. Vibratory compaction was not studied because it is a more advanced process which did not warrant investigation before the basic fuel data were obtained by this project.

*Completed in April 1963. Reported in References 1, 2, 3, 4, 5, 9, and 12.

The advantages and disadvantages of sintering vs arc casting, many of which were not known at the time the project was started, are summarized below.

A. Advantages of Sintering

1. Ease in making small as well as large diameter pellets.
2. Natural subdivision of plutonium, reducing criticality problems.
3. Good control of carbon content.
4. Good plutonium homogeneity.
5. Good dimensional control in the as-sintered condition with the possibility that grinding may be omitted even with a helium contact bond.

B. Disadvantages of Sintering

1. The necessity of handling large quantities of fine particle size, easily oxidizable, pyrophoric powders. This requires high-purity inert handling atmospheres. (For 90% or less of theoretical density, larger particle sizes with less pure atmospheres are possible.)
2. The requirement to fabricate and handle a large number of short pellets.

C. Advantages of Arc Melting

1. Less stringent control of handling atmosphere is required, since carbide powders are not needed.
2. Longer and fewer rods are handled.

D. Disadvantages of Arc Melting

1. Difficulty in making small diameter rods (less than 1/4 in.).
2. Large amounts of Pu that have to be handled, particularly in skull melting, with attendant criticality problems, and high inventory costs.
3. Difficult control of carbon content.

4. Permanent requirement for surface grinding, or the use of a liquid-metal bond with associated compatibility problems.
5. Plutonium losses in vacuum at the high melting temperatures, requiring development of partial pressure techniques.

The sintered and arc cast products differ in several ways. Whether these differences are advantageous or disadvantageous remains to be seen.

1. Higher level of oxygen impurity in the sintered (500 to 4000 ppm) than the arc cast material (700 ppm maximum).
2. Smaller grain size in the sintered material.
3. Somewhat lower achievable density for sintered material (98% of theoretical instead of 99%).
4. A controllable sintered density capable of producing porous fuel if fission gas venting is desirable.

The initial fabrication studies were with UC to establish the basic process parameters. This helped to determine the equipment required in the plutonium glove boxes, shortened the schedule, and reduced the cost of the over-all project by permitting experimental work while the plutonium facility design and construction were in progress.

Work with plutonium was initiated in March 1961.

4.2 UC FABRICATION

4.2.1 Powder Preparation

The first objective was the synthesis of high purity uranium monocarbide (stoichiometric composition 95.2 w/o U and 4.8 w/o C) by heating mixtures of uranium oxides (UO_2 and U_3O_8) and carbon according to the reactions:

$$UO_2 + 3\ C \rightarrow UC + 2\ CO$$

$$U_3O_8 + 11\ C \rightarrow 3\ UC + 8\ CO$$

Stoichiometric mixtures of Mallinckrodt ceramic-grade UO_2 and a commercial carbon produced by cracking natural gas were milled for 24 hr in a rubber-lined ball mill with SS balls and dry pressed at approximately 15,000 psi into pellets about 1 in. in diameter and 1-in. high. The pellets were then reacted at 1750 to 1800°C in a 100-μ vacuum or in argon at atmospheric pressure. Reacting at higher temperatures tended to increase the UC_2 content of the pellets.

The best results were obtained with UO_2 in vacuum. Typical ranges of analyses were:

	w/o	X-Ray Analysis
Total Carbon	4.70 to 4.97	Major UC
Free Carbon	<0.04 to 0.09	Very faint UO_2
Oxygen	0.05 to 0.35	
Nitrogen	0.1	
Iron	0.1	

Reactions with U_3O_8 did not produce as consistent a product and tended to form more UC_2.

Reactions in argon did not produce a consistent product. The argon atmosphere was not sufficiently pure. As a result a specification of 10 ppm (max) oxygen and moisture was established for the helium furnace atmosphere to be used in the (UPu)C synthesis and sintering.

4.2.2 Pellet Preparation

A. Pressing and Sintering

Stoichiometric UC

The object of this investigation was to produce high density (about 95% of theoretical) fuel pellets for evaluation by metallographic, X-ray, and chemical tech-

niques, for cladding compatibility and irradiation studies, preliminary to analogous studies of (UPu)C fuel pellets. To this end several variables in the fabrication process were investigated, including particle size, cold forming pressures, milling time, amount of binder, sintering time, and temperature.

The general procedure was to cold press and sinter fine particle size, UC powder produced by reacting stoichiometric amounts of UO_2 and carbon. The crushed clinker was milled in an argon filled, rubber-lined mill with SS balls. Carbowax 6000, dissolved in trichlorethylene, was used as the temporary binder.

In some of the early experiments, the cold pressed UC pellets were immediately placed into the vacuum induction furnace for sintering. It was found that in the lower temperature ranges this furnace could not be controlled sufficiently to remove the temporary binder without damage to the pellet. Consequently, a procedure was adopted to heat the pellets slowly to about 1500°C in a ceramic tube furnace using an argon atmosphere and SiC heating elements to remove the temporary binder. The sintering was completed at higher temperatures in a vacuum induction furnace. The (UPu)C compacts were subsequently sintered in a graphite-pin resistance furnace, in one firing, since such a furnace has the capabilities of achieving high temperatures and of accurately controlling the temperature ranges.

In most of the experiments described in this section, the pellets were placed in graphite crucibles for sintering. Near the end of the study it was found that tantalum-lined graphite crucibles were superior because they avoided the direct contact of the pellets with the graphite and therefore removed any tendency to form UC_2 on the surface of the pellets.

The size of the pellets needed for irradiation studies was 0.191 ± 0.001-in. diameter by about 0.2-in. long. Most of the pellets described in this section were of these approximate dimensions.

In order to determine the best amount of Carbowax 6000 to use as a temporary binder, pellets were fabricated with 1/4, 1/2, and 3/4% additions, using 16,000 psi as the forming pressure. Although the data in Table 4.1 indicate little effect, the pellets with 1/2% Carbowax had sufficient strength for easy handling and this is probably the best amount to use.

The effect of particle size and temperature on sintered density is indicated in Table 4.2. In these experiments, the pellets were cold pressed at 40,000 psi with 1/2% Carbowax binder. A considerable improvement in sintered density was obtained by decreasing the particle size. Subsequent studies were made with the fine particle size material.

Table 4.3 indicates the results of a study on the effects of temperature and time on density and structure. In these experiments, the cold forming pressure was 16,000 psi and the temporary binder was 1/2% Carbowax 6000. The UC powder had been milled for 36 hr. The longer sintering times and higher temperatures increased the tendency to form UC_2 and decreased the UO_2 content without an improvement in sintered density.

The effect of milling time on both unfired and sintered density is indicated in Table 4.4. A forming pressure of 16,000 psi was used with the pellets, which were sintered for 1 hr at 1850°C. It was noted that increasing the milling time from 24 to 72 hr did not improve the sintered density.

Table 4.5 indicates the effect of forming pressure on unfired and final pellet density. The UC was ball milled for 36 hr. The sintering was in a vacuum for 1 hr at 1800°C. Although there was a gradual increase in unfired density going from 15,000 to 30,000 psi forming pressures, there was no significant trend in sintered densities.

TABLE 4.1 — EFFECT OF BINDER PERCENTAGE ON DENSITY OF UC

Carbowax, %	1/4	1/2	3/4
Green Bulk Density, g/cm^3	8.59	8.75	8.44
Sintered Bulk Density, g/cm^3	12.40	12.83	12.53

TABLE 4.2 — EFFECT OF PARTICLE SIZE ON DENSITY OF UC

Particle Size	Density, g/cm^3 1850°C	1950°C	2050°C	X-Ray Analysis	Chemical Analysis, w/o	
-80 mesh	—	10.30	9.93	—	—	
2 μ	—	10.65	10.60	—	—	
0.5 μ*	12.50	—	—	Major phase, UC	U	94.96
				Minor phase, UC_2	Total C	5.29
					Free C	0.04
					Fe	0.04
					N	0.10

*The fine particle size was obtained by increasing the ball milling time to 24 hr from the previously used 4 hr.

TABLE 4.3 — EFFECT OF TIME AND TEMPERATURE OF SINTERING ON DENSITY OF UC PELLETS

Temp, °C	Sintering Time, hr	Density, g/cm^3	X-Ray Analysis
1750	1	11.85	Major UC, very faint UO_2
1850	1	12.49	Major UC, very faint UO_2 and UC_2
1850	3	12.22	Major UC, weak to moderate UC_2
2100	1/2	12.42	Major UC, weak to moderate UC_2

TABLE 4.4 — EFFECT OF MILLING TIME ON DENSITY OF UC

Milling Time, hr	24	48	72
Green Bulk Density, g/cm^3	8.75	8.70	8.80
Sintered Bulk Density, g/cm^3	12.83	12.67	12.69

TABLE 4.5 — EFFECT OF FORMING PRESSURE ON UNFIRED AND FINAL UC PELLET DENSITY

Forming Pressure, psi	Unfired Density, g/cm^3	Fired Density, g/cm^3
15,000	8.76	11.21
20,000	8.87	10.95
30,000	9.02	11.29
40,000	9.02	11.11

Two larger batches of pellets were made for evaluation by chemical analysis, X-ray diffraction, metallography, hardness, and fuel-cladding interaction studies. Densities of up to 95% of theoretical were achieved. The fabrication process used and the results are indicated in Table 4.6.

Metallography of samples from both batches of pellets indicated a structure of UC with a small amount of UC_2. A small amount of oxygen is in solid solution.

Diamond pyramid hardness readings with 15 kg (superficial Rockwell), 1 kg (New-age microhardness), and 200 g (Bergman microhardness) produced a scatter greater than would be expected from UC alone. Cracking and porosity were the probable causes of the scatter. Microhardness readings with 100 and 200-g loads gave reproducible values that averaged 600 Vickers hardness. The 200-g loads caused hairline cracks.

UC with Sintering Aid

Compatibility tests between Inconel-X and UC (Section 5.3) showed solubility of nickel in UC. This indicated that nickel might be a sintering aid for UC in much the same way as nickel and cobalt are sintering aids to WC. WC-Co compacts are generally sintered at 1400°C, which is 80°C above the WC-Co eutectic. A WC-Co liquid solution is formed which dissolves some of the WC grain boundaries and produces dense packing of the carbide phase. Upon cooling, WC crystals are precipitated from the liquid phase. An attempt was made to simulate this with nickel and UC.

The first experiments used additions of 5% nickel to UC. Nickel reduced the required sintering temperature by 200°C for 86% dense pellets, but did not improve the ultimate density.

Additional sintering experiments were next carried out using smaller amounts of nickel with a longer holding time. The sintering was done in a ceramic tube fur-

TABLE 4.6 — FABRICATION PROCEDURE AND PROPERTIES OF UC PELLETS

Item	Batch No. 1	Batch No. 2
Milling time, hr	24	24
Particle size, μ	~1	<1
Binder, % Carbowax	1/4	1/4
Cold pressing pressure, psi	16,000	16,000
Pre-sintering		
Temp, °C	1750	1500
Time, hr	1	1
Atmosphere	Argon	Argon
Final sintering		
Temp, °C	1850	1850
Time, hr	1	1
Atmosphere	100 μ vac	100 μ vac
No. of pellets	14	15
Density		
Range		
g/cm^3	12.2-12.5	12.4-13.0
% of theoretical	89.5-91.8	91.3-95.5
Average		
g/cm^3	12.3	12.7
% of theoretical	90.4	93.3

Chemical Analysis		Lowest Density	Highest Density
U, w/o	94.87	95.01	94.94
Total C, w/o	4.71	4.62	4.58
Free C, w/o	0.05	0.03	0.03
Fe, w/o	0.01	—	—
N, w/o	<0.10	0.09	by vacuum fusion
O, w/o	~0.25, by difference	0.35	by vacuum fusion
X-ray diffraction	Major, UC Faint, UC_2 Faint, UO_2	Major, UC Faint, UC_2 Very faint, UO_2	Major, UC Faint, UC_2 Very faint, UO_2
Lattice constant, Å	4.963 ± 0.001	4.963 ± 0.002	

nace in a helium atmosphere. Temperature was raised at the rate of about 50°C per hour to 1000°C to remove temporary binder and then was raised rapidly (in about 1/2 to 1 hr) to the sintering temperature.

The results are summarized in Table 4.7. The optimum temperature indicated is 1525°C, while 0.1 w/o nickel is as effective as the larger amounts. With 1.0 w/o nickel there was some tendency for the pellets to react with the tantalum crucible at 1600°C and higher. This was not observed when smaller amounts (0.5 and 0.1 w/o) of nickel were used.

Metallographic examination of the UC-Ni compacts showed a UC + U_2C_3 structure. Microhardness of UC was 640 VPH and that of U_2C_3 was 560 VPH.

UC with Excess Metal

Some experiments were conducted to determine if excess uranium metal in the uranium carbide would be a sintering aid. Three approaches were taken: addition of metal directly to the uranium carbide, synthesizing uranium carbide by the uranium dioxide-carbon reaction with a deficiency of carbon, and the addition of uranium to the uranium carbide as the hydride and then converting the hydride to the metal. The final pressing and sintering of the pellets was by the previously described method. No marked improvement in fuel density was achieved.

B. Hot Pressing UC Powder

Two experiments were carried out to determine if UC pellets of nearly theoretical density could be obtained by hot pressing in an aluminum nitride mold. The maximum density obtained was 12.4 g/cm^3, which was less than desired. The reaction with the aluminum nitride was slight. Previous experimenters and experience on this project had shown that UC reacts with graphite molds at the hot pressing temperatures to form UC_2.

TABLE 4.7 — EFFECT OF ADDITIONS OF SMALL AMOUNTS OF NICKEL ON THE SINTERING OF UC*
(Theoretical Density of UC is 13.63 g/cm^3)

Time at Sintering Temperature, 4 hr

Experiment No.	Amount of Ni, w/o	Sintering Temp, ℃	Density, g/cm^3 With Ni	Density, g/cm^3 Without Ni	X-Ray Analysis
1	1.0	1350	10.2	8.5	
2	1.0	1450	12.2	8.5	
3	1.0	1485	12.75	9.15	
4	1.0	1525	12.87	9.28	Major UC type
5	1.0	1600	12.7†	10.2	Faint U_2C_3 type
6	1.0	1800	12.7†	11.0	Faint UO_2
7	0.5	1485	12.9	9.15	(After 1800℃
8	0.5	1525	12.98	9.28	sintering U_2C_3
9	0.1	1485	12.40	9.15	was not detect-
10	0.1	1525	12.98	9.28	able)
11	0.1	1600	12.75	11.45	
12	0.1	1800	12.60	12.35	

*Analysis of UC: U, 95.12 w/o; total C, 4.64 w/o; free C, 0.06 w/o; N, <0.05 w/o; Fe, <0.01 w/o.
†Tendency to react with tantalum crucible.

4.3 (UPu)C FABRICATION

4.3.1 Powder Preparation

The preparation of (UPu)C powder was studied by four methods:

1. $PuO_2 + 3\ C \rightarrow PuC + 2\ CO$

   $4\ UC + PuC \rightarrow 5\ (U_{0.8}Pu_{0.2})C$
2. $2\ PuO_2 + 7\ C \rightarrow Pu_2C_3 + 4\ CO$

   $Pu_2C_3 + U + 7\ UC \rightarrow 10\ (U_{0.8}Pu_{0.2})C$
3. $4\ UO_2 + PuO_2 + 15\ C \rightarrow 5\ (U_{0.8}Pu_{0.2})C + 10\ CO$
4. $5\ (U_{0.8}Pu_{0.2})O_2 + 15\ C \rightarrow 5\ (U_{0.8}Pu_{0.2})C + 10\ CO$

Starting materials were as follows:

PuO_2	Prepared by Dow Chemical Company Rocky Flats Plant by the oxidation of the metal, total impurities: <400 ppm; particle size: -200 mesh; O/Pu ratio: 2.015.
UO_2	Prepared by United Nuclear Corporation, Chemicals Division, total impurities: <200 ppm; O/U ratio: 2.05.
$(U_{0.8}Pu_{0.2})O_2$	Prepared by the coprecipitation of the peroxides and calcining by General Electric Co., Hanford Atomic Products Operations. Total impurity content was about 5000 ppm with Ca, Cr, Cu, and Fe being present in excess of 500 ppm each; particle size: -200 mesh.
C	A commercial product prepared by the cracking of methane. Particle size about 0.1μ; ash content of 0.05%.

The general procedure used in preparing the oxide-carbon mixtures for reaction was as follows. The oxide and calculated weight of carbon were dry ball-milled for 24 hr in a rubber-lined mill with stainless steel balls. The mixture was pressed at 5000 psi, without binder, into pellets 0.6 in. in diameter by about

0.6-in. high, after which each pellet was cut by a thin spatula into pieces of approximately equal size. Batches of about 10 to 50 g of the pellets were then heated in a graphite crucible in a graphite resistance furnace with a helium atmosphere. During the heating period, helium was aspirated through the furnace at the rate of 30 liters per minute to carry off the carbon monoxide formed in the reaction. The helium atmosphere purity was <10 ppm oxygen and moisture. A Mine Safety Appliance Corporation type carbon monoxide tester, connected to the exhaust line from the furnace, monitored the end of the reaction.

A. PuC + UC

The initial plan, process No. 1, was that PuC would be prepared in the plutonium facility, UC would be prepared outside the plutonium facility, and the two would then be mixed, pressed, and sintered to form pellets. Attempts to produce single-phase PuC by the carbothermic reduction of the oxide were unsuccessful. The products, produced at temperatures ranging from 1300°C to the melting point of PuC (about 1650°C), all contained at least two major phases. The difficulty of producing PuC by this route was confirmed by other laboratories. As a result, further work on this process was stopped.

B. Pu_2C_3 + U + UC

Single-phase Pu_2C_3 was prepared easily by reacting PuO_2 and carbon at 1550°C for 5 hr. The product contained 7.11 to 7.16 w/o C (theoretical is 7.00 w/o C). X-ray analysis showed single-phase Pu_2C_3 with a lattice parameter of 8.133 Å.

Since Pu_2C_3 was readily synthesized, it was used to prepare (UPu)C. Pu_2C_3 was reacted with sufficient UC and U metal powders to give the desired U/Pu ratio in the (UPu)C product. The results of the experiments are summarized in Table 4.8. A moderately good grade of (UPu)C was produced by this method. However, work was abandoned on this method because the powder preparation

TABLE 4.8 — SUMMARY OF EXPERIMENTS ON THE PREPARATION OF (UPu)C SOLID SOLUTIONS FROM UC* + Pu_2C_3 + U
(Stoichiometric Carbon Content is 4.80 w/o)

Experiment No.	Reaction	Reaction Temp, °C	Hold Time, hr	Chemical Analysis, w/o			X-Ray Analysis
				Pu+U	C	Pu+U+C	
1	$U + Pu_2C_3 \longrightarrow (U_1Pu_2)C_3$	1100 1450	1 1	94.0	5.05	99.05	Single phase (UPu)C type
2	$7\ UC + U + Pu_2C_3 \longrightarrow (U_8Pu_2)C_{10}$	1100 1450	1 1	94.0	4.83	98.83	Major (UPu)C type Trace $(UPu)O_2$ type
3	$7\ UC + U + Pu_2C_3 \longrightarrow (U_8Pu_2)C_{10}$	1100 1450	1 1	94.53	4.87	99.40	Major (UPu)C Weak $(UPu)_2C_3$ Faint $(UPu)O_2$
4	Product from "3" crushed, milled, and reheated	1700	1	94.37	4.79	99.16	Major (UPu)C Faint $(UPu)_2C_3$ $a = 4.965 \pm 0.001$ Å

*Analysis of UC: U, 95.0 w/o; C, 4.72 w/o.

required two steps and offered no advantages over the single-step $UO_2 + PuO_2 + C$ method being developed in parallel.

C. $UO_2 + PuO_2 + C$

Single-phase $(U_{0.8}Pu_{0.2})C$ was prepared by reacting UO_2, PuO_2, and C in the temperature range of 1500 to 1700°C. To study the effect of carbon stoichiometry on the carbide powder structure, reaction mixes were made containing 100, 95, and 90% of the stoichiometric carbon, reacted at 1500°C for 3 hr, and then 1700°C for 1 hr. The results indicated that the material with 95% of theoretical carbon was the most desirable, since no sesquicarbide phase was formed as indicated by X-ray analysis. Table 4.9, experiment No. 2, shows the results obtained with the preferred carbon content. Lower carbon material may produce an undesirable zeta phase.

To determine the best synthesis temperature, mixes were heated to 1550°C with hold times of 5 to 8 hr, followed by heating to 1625 and 1700°C with hold times of 1 to 2 hr. Reacted pellets were crushed and repelletized before each reheat. The results of these experiments [along with companion $(UPu)O_2 + C$ experiments summarized in Table 4.10] indicate that an essentially single-phase material can be produced from either method at about 1625°C. Subsequent synthesis of carbide powders for irradiation specimens (Section 3.3.2) and property measurements (Section 5 and Reference 22) substantiated this conclusion.

Since the mechanically mixed oxide route was simpler, it was adopted as the method for synthesis of carbide powders for future work.

An accurate, reliable method was found to determine the completion of the reaction in the synthesis of carbide powders. A Mine Safety Appliance Corporation type carbon monoxide tester was connected to the exhaust line from the furnace and the gas was sampled periodically. Carbon monoxide, in a concentration of

TABLE 4.9 — THE EFFECT OF CARBON CONTENT ON THE SYNTHESES OF (UPu)C POWDERS

(Synthesized 1500°C-3 hr; 1700°C-1 hr)

Experiment No.	Intended Composition	Carbon, w/o	X-Ray Analysis
1	$(U_{0.8}Pu_{0.2})C_{1.0}$	5.05	Major (UPu)C Weak $(UPu)_2C_3$ (There appears to be a double UC-type phase)
2	$(U_{0.8}Pu_{0.2})C_{0.95}$	4.63	Single-phase (UPu)C $a_0 = 4.964 \pm 0.001$ Å
3	$(U_{0.8}Pu_{0.2})C_{0.90}$	4.75	Single-phase (UPu)C $a_0 = 4.964 \pm 0.001$ Å

TABLE 4.10 — RESULTS OF ADDITIONAL EXPERIMENTS TO PRODUCE $(U_{0.8}Pu_{0.2})C_{0.95}$ BY CARBON REDUCTION OF THE OXIDES

Experiment No.	Starting Material	Reaction Temperature, Time, and Total Carbon: 1550°C 5-hr Hold	1550°C 8-hr Hold	1625°C +1-hr Hold	1625°C +1-hr Hold	1700°C +1-hr Hold
1	UO_2, PuO_2, C	6.94	—	5.00	4.53*	—
2	$(UPu)O_2$, C	—	4.75†	4.75‡	—	4.44§

*Major (UPu)C; faint $(UPu)O_2$ and $(UPu)_2C_3$ a = 4.968 ± 0.001 Å.
†Major (UPu)C; faint $(UPu)_2C_3$; weak $(UPu)O_2$.
‡Major (UPu)C; faint $(UPu)O_2$.
§Major (UPu)C; very faint $(UPu)O_2$.

0.000 to 0.007%, indicated the completion of the reaction. This is approximately the CO concentration in the exhaust gas from the heated empty furnace. The result of several synthesis experiments monitored with the CO indicator are shown in Table 4.11. Theoretical carbon for these compositions is 4.55 w/o.

D. $(UPu)O_2 + C$

Essentially single-phase $(U_{0.8}Pu_{0.2})C$ was prepared by reacting solid solution mixed oxides with carbon in the temperature range 1550 to 1700°C. The results are compared to those achieved with mixed oxides in Table 4.10.

It was hoped that solid solution oxide starting materials would avoid or minimize sesquicarbide formation. The theory was generally borne out, but results were not conclusive because of sporadic reactions with the tantalum crucible liners. The reactions were thought to be caused by the high impurity level in the $(UPu)O_2$. Work on this process was discontinued because of the good results obtained with the simpler process using mechanically mixed oxides.

4.3.2 Pellet Preparation

Using the information obtained in the UC and UC-Ni work as a guide, sintering experiments were made on $(U_{0.8}Pu_{0.2})C$ powder. The pellets, approximately 0.2 by 0.2 in., were prepared by ball milling the powder in a rubber-lined mill with stainless steel balls for 24 hr, mixing it with 1/2% Carbowax 6000 dissolved in trichlorethylene and cold pressing at 30,000 psi. If sintering aid was desired, it was added during the ball milling step. The pellets were sintered in a tantalum-lined graphite crucible in a helium atmosphere containing <10 ppm of oxygen and moisture. Starting material made by the mixed oxide method and the Pu_2C_3 method were compared. UC control specimens were carried along.

The results are presented in Table 4.12. The effectiveness of the nickel sintering aid was again demonstrated. The best density for the solid solution was achieved

TABLE 4.11 — RESULTS OF SYNTHESIS EXPERIMENTS AT 1625°C TO PRODUCE $(U_{0.8}Pu_{0.2})C_{0.95}$ (MONITORED BY CO METER)

Experiment No.	Batch Size, g	CO at End of Run, %	Time to Reach Respective % CO,* hr	Total Carbon, %	X-Ray Analysis
1	50	0.005	6½	4.53	Single-phase (UPu)C $a_0 = 4.965 \pm 0.001$ Å
2	15	0.007	2½	4.58	Single-phase (UPu)C $a_0 = 4.965 \pm 0.001$ Å
3	50	0.005	7½	4.61	Major (UPu)C Faint $(UPu)O_2$ $a_0 = 4.965 \pm 0.001$ Å
4	50	0.005	5½	4.60	Single-phase (UPu)C $a_0 = 4.969 \pm 0.001$ Å

*Note that smaller batches required less time for completion.

TABLE 4.12 — EFFECT OF NICKEL ADDITION ON THE SINTERING OF UC* AND (UPu)C
(Theoretical Density of the Carbides is 13.6 g/cm^3)

Experiment No.	Sintering Temp, °C	Material and Density, g/cm^3					
		UC	UC+0.1% Nickel	$(U_{0.8}Pu_{0.2})C_{0.95}$	$(U_{0.8}Pu_{0.2})C_{0.95}$ + 0.05% Ni	$(U_{0.8}Pu_{0.2})C_{0.95}$ + 0.1% Ni	$(U_{0.8}Pu_{0.2})C_{0.95}$ + 0.2% Ni
1†	1350	8.48	11.40	10.07	–	12.26	–
1a‡				9.56	11.59	12.24	12.31
2†	1450	8.56	12.75	10.61	–	12.75	–
2a‡				9.89	12.05	12.59	12.78
3†	1550	9.44	12.65	11.77	–	12.97	–
3a‡				11.77	12.49	12.83	12.78
4†	1650	9.48	12.55	12.00	–	12.75	–
4a‡				12.10	12.33	12.72	12.76
5†	1750	10.37	12.69	–	–	12.81	–
5a‡				12.20	12.45	12.75	12.68

*Analysis of UC: U, 95 w/o; C, 4.72 w/o.

†$(U_{0.8}Pu_{0.2})C_{0.95}$ solid solution synthesized from carbon reduction of the oxides to form the composition $(UC_{0.8}PuC_{0.2})C_{0.95}$.

‡$(U_{0.8}Pu_{0.2})C_{0.95}$ solid solution synthesized from the reaction of 7 UC + U + Pu_2C_3 to form a stoichiometric composition.

with 0.1% Ni addition, sintered at 1550°C. The density was 95% of theoretical. The carbide powder made by the mixed oxide method sintered to slightly higher densities. Since the mixed oxide method of synthesis is also more economical than the Pu_2C_3 method, the mixed oxide method was adopted as the one to be used in future syntheses.

The results of previous work on UC at The Carborundum Company indicated free carbon hindered densification. Therefore, small additions of free carbon were made to study its effect on the sinterability of $(U_{0.8}Pu_{0.2})C_{0.95}$ compacts containing 0.12% nickel. Results appear in Table 4.13. The nickel sintering aid appeared to be less effective in the pellets containing as little as 0.10 w/o additional free carbon.

Only a limited amount of work was done under this contract on sintering $(U_{0.8}Pu_{0.2})C_{0.95}$ without sintering aids as shown in Table 4.12. The highest density was 12.2 g/cm^3 (89.5% of theoretical) achieved at the highest sintering temperature, 1750°C.

Additional sintering experiments under Contract AT(30-1)-3118 (Reference 22) showed that densities as high as 12.8 g/cm^3 could be attained by sintering at 1925°C. Chemical analyses indicated that within experimental error, the uranium-to-plutonium ratio had not been changed by the high temperature sintering. Plutonium would vaporize at a greater rate than uranium; therefore, it was concluded that plutonium was not vaporizing, and the fabrication procedure was adopted to produce pellets without sintering aid for the irradiation specimens (Section 6.3.2).

TABLE 4.13 — THE EFFECT OF NICKEL AND CARBON ADDITIONS ON SINTERING OF $(U_{0.8}Pu_{0.2})C_{0.95}$

Experiment No.	Composition of Pellet	Temperature and Hold Time	Average Density, g/cm³	Total Carbon, %	X-Ray Analysis
1	$(U_{0.8}Pu_{0.2})C_{0.95}$	1550°C with a 1/2-hr hold	10.81	4.64	Major (UPu)C Faint $(UPu)_2C_3$
2	$(U_{0.8}Pu_{0.2})C_{0.95}$ + 0.12 w/o Ni		12.90	4.68	Single-phase (UPu)C* a_0 = 4.9644 ± 0.0003 Å
3	$(U_{0.8}Pu_{0.2})C_{0.95}$ + 0.12 w/o Ni + 0.10 w/o C		12.72	4.76	
4	$(U_{0.8}Pu_{0.2})C_{0.95}$ + 0.12 w/o Ni + 0.20 w/o C		12.74	4.88	
5	$(U_{0.8}Pu_{0.2})C_{0.95}$	1550°C with a 1-hr hold	11.83	4.60	Major (UPu)C Faint $(UPu)_2C_3$
6	$(U_{0.8}Pu_{0.2})C_{0.95}$ + 0.12 w/o Ni		12.91	4.77	Major (UPu)C Faint $(UPu)_2C_3$ a_0 = 4.9644 ± 0.0002 Å
7	$(U_{0.8}Pu_{0.2})C_{0.95}$ + 0.12 w/o Ni + 0.10 w/o C		12.68	4.83	Major (UPu)C Weak $(UPu)_2C_3$ a_0 = 4.966 ± 0.001 Å
8	$(U_{0.8}Pu_{0.2})C_{0.95}$ + 0.12 w/o Ni + 0.20 w/o C		12.75	4.94	Major (UPu)C Weak $(UPu)_2C_3$ a_0 = 4.949 ± 0.009 Å

*Metallographic examination showed a two-phase structure. X-ray analysis was apparently not sufficiently sensitive to pick up the second phase.

4.4 MISCELLANEOUS FABRICATION

4.4.1 Fabrication of $(UPu)_2C_3$

A. Synthesis

The sesquicarbides may have potential advantages over the monocarbides. Preliminary experiments were started to obtain some information on the fabrication technology and properties of the compound, as well as its metallographic and X-ray characterization.

Two experiments were performed to synthesize $(U_{0.8}Pu_{0.2})_2C_3$. Stoichiometric proportions of PuO_2, UO_2, and carbon were blended and cold compacted, without binder, at 30,000 psi. The reaction pellets were heated to 1650°C with a hold time of 4 hr. Chemical analyses on the pulverized products gave total carbon at 6.95 to 6.98 w/o. The theoretical carbon content is 7.02 w/o. The results of X-ray analyses showed a major $(UPu)_2C_3$ phase, a faint UC-type structure, and a faint phase which could not be identified. The unit cell size for the sesquicarbide phase was $a_0 = 8.108 \pm 0.002$ Å. The ASTM index card lists $a_0 = 8.129$ for Pu_2C_3 and $a_0 = 8.088$ for U_2C_3.

B. Pelletizing

Several sintering experiments were performed with the 25-g batch of sesquicarbide powder. For this purpose, the pulverized product was milled for 24 hr in a rubber-lined mill using stainless steel balls.

Pellets for the initial sintering experiment were cold pressed without a binder. The resulting pellets were laminated badly after sintering. Pellets fabricated for subsequent sintering experiments were made with 1/4 w/o Carbowax binder and cold pressed in the usual manner at 30,000 psi. The pellets were 0.225 in. in diameter and about 0.2-in. long. Three experiments were carried out with these

pellets. The sintering temperatures were 1650, 1700, and 1750°C with hold times of 1 hr. The results are shown in Table 4.14.

The cause for the cracking of the pellet during the 1750°C sintering is not known. The structure of the 1750°C sintered pellet is shown in Fig. 4.1.

4.4.2 Fabrication of (UPu)(OC)

Several experiments were performed in an attempt to synthesize $(U_{0.8}Pu_{0.2})(OC)$ and Pu(OC). The existence and stability of the pure, mixed monoxide phase were unknown. However, the existence of a carbon stabilized (UPu)O was very likely. The identification of (UPu)(OC) type compounds is important, since there are significant quantities of oxygen present in the (UPu)C produced by the oxide-carbon reaction. In addition, such a compound could have desirable engineering properties: improved oxidation resistance over the pure carbide and the equivalent thermal conductivity.

For reaction purposes UO_2, PuO_2, and C in stoichiometric proportions to give $(U_{0.8}Pu_{0.2})O$ were intimately blended and pressed, without binder, into 0.2-in. diameter pellets. The forming pressure was 30,000 psi.

For synthesis, the temperatures investigated were 1650, 1750, 1850, 1950, and 2000°C.

Metallographic examination of a typical product showed a two-phase structure, a gray dioxide-type phase, and a light monoxide-type phase, each about 50% in volume. (See Fig. 4.2.)

The method of synthesis produced a product of about 1 w/o carbon containing a mixture of dioxide- and monoxide-type phases. The carbon distribution between the two phases was unknown.

TABLE 4.14 — RESULTS OF SINTERING EXPERIMENTS WITH $(U_{0.8}Pu_{0.2})_2C_3$

Experiment No.	Sintering Temp, °C	Time, hr	Sintered Density*	Total Carbon,† w/o	X-Ray Analysis
1	1650	1	11.80-11.90 (11.83 avg)	6.84	Major $(UPu)_2C_3$ Faint (UPu)C
2	1700	1	11.95-12.05 (12.00 avg)	6.75	Major $(UPu)_2C_3$ Faint (UPu)C
3	1750	1	Pellet cracked	6.90	Camera Major $(UPu)_2C_3$ Faint (UPu)C $a_0 = 8.089 \pm 0.004$ Å Diffractometer Major $(UPu)_2C_3$ $a_0 = 8.08997 + 0.00009$ Å $- 0.00006$ Å Moderate (UPu)C $a_0 = 4.959 \pm 0.002$ Å Weak/moderate $(UPu)C_2$

*Theoretical density for Pu_2C_3 is 12.7 g/cm^3 and 12.68 g/cm^3 for U_2O_3.
†Theoretical carbon content is 7.02 w/o.

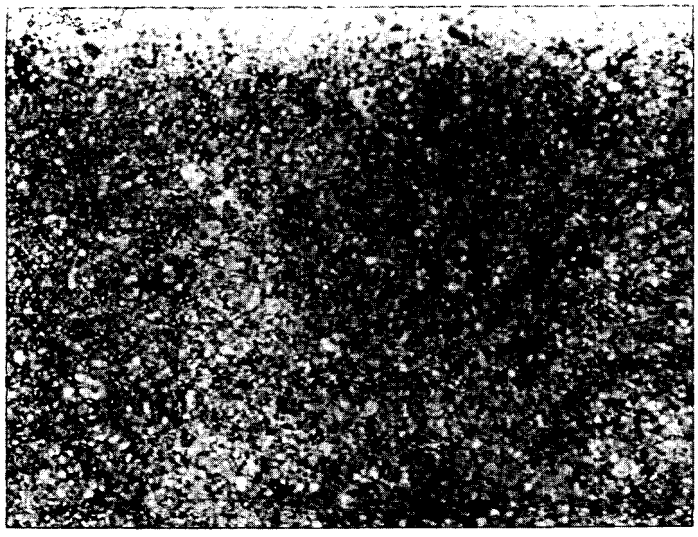

150×

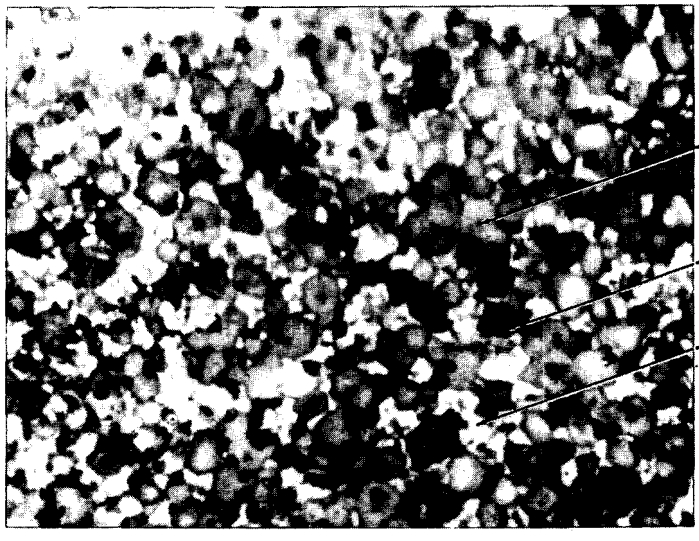

600×

Fig. 4.1 — Solid Solution Sesquicarbide $(U_{0.8}Pu_{0.2})_2C_3$. Pellet Sintered at 1750°C, 1 hr. Etchant: Nitric Acid-Lactic Acid-Water.

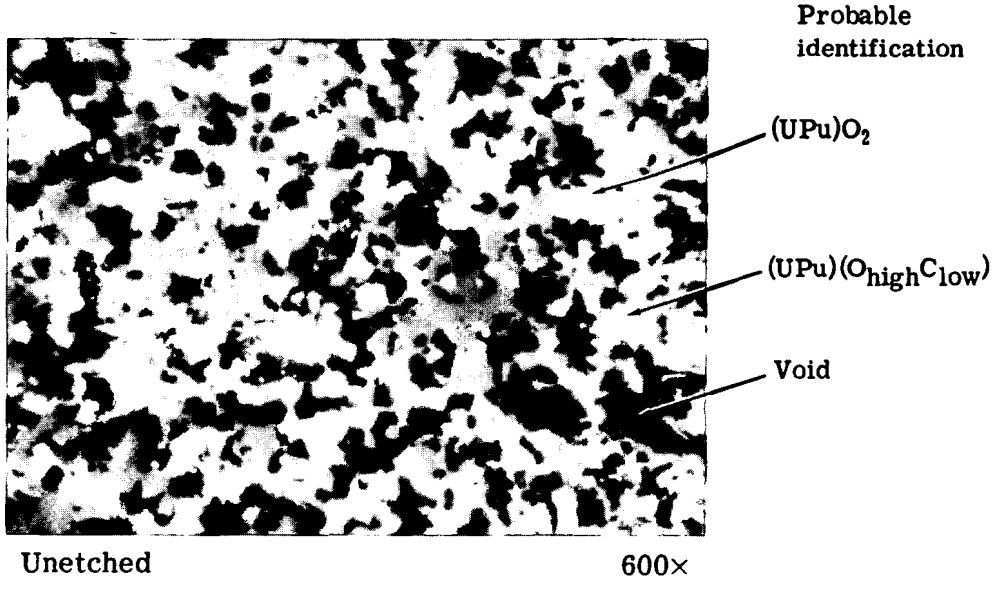

Fig. 4.2 — Reaction Product from $(U_{0.8}Pu_{0.2})(OC)$ Synthesis. Heated 1850°C – 6 hr; 2000°C – 1 hr.

5. FUEL PROPERTIES*

5.1 INTRODUCTION

The objective of the out-of-pile property measurements was to study the characteristics of (UPu)C which have the most significant effect on its operational behavior.

1. Structural Characterization

   The identification of the fuel structure is a basic necessity to interpret the properties and behavior of the fuel

2. Fuel-Cladding Compatibility

   Minimum fuel-cladding reactions are desirable to prevent fuel diffusion through the cladding and to prevent deterioration of the cladding properties.

3. Coefficient of Expansion

   Knowledge of the thermal expansion behavior is necessary to evaluate the fuel-cladding gap at operating conditions

4. Melting Point

   A high melting point is desirable to minimize fission gas release and maximize dimensional stability.

*Completed in April 1964. Reported in References 2, 3, 4, 5, 6, 8, 12.

5. Thermal Stability and Vapor Pressure

A high thermal stability is desirable to prevent fuel decomposition and chemical reaction of the fuel at high temperatures.

The structural characterization was studied on the 20% PuC composition. The other property measurements were made on a 5% PuC composition. Similar property measurements were made on a 20% PuC composition under a Joint USAEC-Euratom sponsored contract and they are reported in Reference 22.

5.2 STRUCTURAL CHARACTERIZATION

5.2.1 Metallography and Microprobe Analyses of Fuel

A. Metallography

Carbide pellets were sectioned and ground with diamond tools, and drilled and measured with tungsten carbide tools under cutting oil. In this way, oxidation of the sample and the pyrophoricity hazard were reduced. Specimens were mounted for metallography by casting and setting in a polyester resin.

The specimens were ground for metallography with successive 180-, 340-, and 600-grits of SiC and kerosene lubricant, followed by polishing with 7, 3, and 1 μ diamond paste with DP lubricant. The procedure was subsequently simplified to grinding with 180- and 600-grit SiC with kerosene lubricant followed by polishing on a Syntron vibrator with 0.3 μ Al_2O_3 (Linde A).

All of the metallographic preparation was done in a nitrogen atmosphere with a maximum of 500 ppm oxygen. The moisture content was higher because of the many solutions used in the glove boxes.

The basic etchant used was the standard nitric acid-acetic acid-water solution. The standard proportions of one-third of each component used for UC usually

etched the (UPu)C too rapidly. To slow down the reaction, mixtures as low as 15% nitric acid, 15% acetic acid, and 70% water were used. The best proportions often had to be adjusted to the specific sample being etched. The monocarbide structure was colored in various hues from straw yellow to red or light blue to purple. Sesquicarbide, dicarbide, uranium, and plutonium metal were left white and unetched.

A 10% bromine-90% anhydrous alcohol etch was used to differentiate between metal and higher carbides. The etchant dissolved the metal phase while it left the higher carbides unattacked.

Differentiation between sesquicarbide and dicarbide by etchants is more difficult. Continued etching with the nitric-acetic etch turns the dicarbide a straw color, but this leaves some room for interpretation. The more positive differentiation was made by a combination of the physical shape of the phase (dicarbide is generally in Widmanstätten platelets, and sesquicarbide in more massive forms in grains or on grain boundaries), X-ray diffraction, and specimen history.

Oxides are identified as a gray inclusion in the as-polished, unetched specimen .

B. Microprobe Analyses

Introduction

In the fabrication studies, nickel in amounts as small as 0.1% was found an effective sintering aid for both UC and (UPu)C, making possible the production of pellets of 95% (min) theoretical density. The use of nickel led to significant quantities of a second phase.

Microprobe analyses, in conjunction with X-ray diffraction and metallographic examination of the UC and (UPu)C specimens, were made to determine the structure of the second phase and the location of the nickel in the crystal structure. Microprobe analyses on UC were made by Advanced Metal Research Corporation

and on (UPu)C by the Monsanto Research Corporation's Mound Laboratory. As the result of this work and the X-ray and metallographic studies, it was concluded that the second phase was sesquicarbide, the nickel was in solid solution in the monocarbide phase, and that no U_xNi_y type compounds were present in the as-sintered specimen.

UC + 0.1% Ni

UC with nickel additions was sintered at 1500 to 1550°C, a temperature at which U_2C_3 is stable (Fig. 5.1). One test to determine whether the second phase was the suspected U_2C_3 was to heat the specimen to 1850°C. This is a temperature where U_2C_3 would decompose peritectoidally to UC and UC_2. Fig. 5.2 shows the predicted transformation occurred. Holding the specimen from 24 to 72 hr at the sintering temperature did not change the structure.

Microprobe analyses were made on the as-sintered and the sintered and reheated specimens. The results are shown in Figs. 5.1 and 5.2. The light phase in the as-sintered specimen (Fig. 5.1) is U_2C_3, with virtually no nickel in solution. The dark phase is conclusively UC with all of the present nickel in solution. Nickel was not found as a metal or intermetallic compound.

The light phase in the sintered specimen reheated to 1850°C in vacuum (Fig. 5.2) is very probably UC_2, and the gray phase is thought to be U_3O_8. Virtually no nickel is in solution in either phase. Although spectral records were obtained on the white and gray phases, no additional detectable elements were noted. The dark phase is conclusively UC with about half the nickel still in solution. The remainder of the nickel has migrated to the grain boundaries, and some has evaporated. Concentrations in excess of 40 to 50 w/o Ni were detected at the interface of the white, gray, and matrix phases. The nickel-enriched regions were much smaller than the electron beam size employed (the beam was 1 to 2 μ) implying even greater concentrations of nickel than noted. Subsequent vacuum annealing

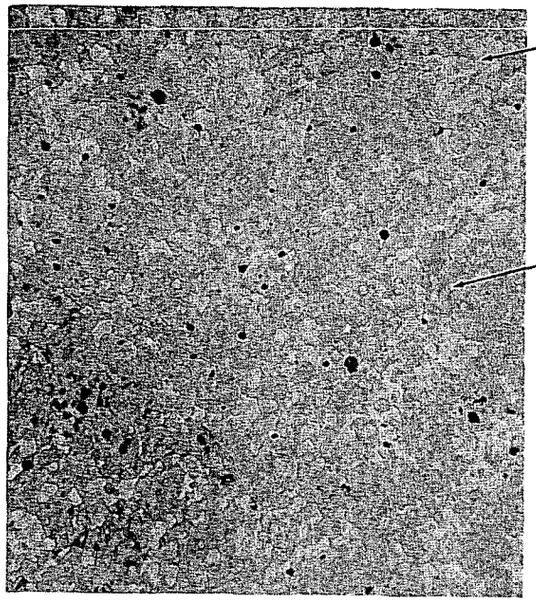

Fig. 5.1 — UC-0.1% Ni – Sintered at 1525°C, 4 hr.
500×. Etchant: Nitric Acid-Acetic Acid-Water.

X-ray identification

Major UC
Minor U_2C_3
Minor UO_2
One strong Ni type line
a_0 = 4.96 Å (breadth of lines
did not allow greater precision)

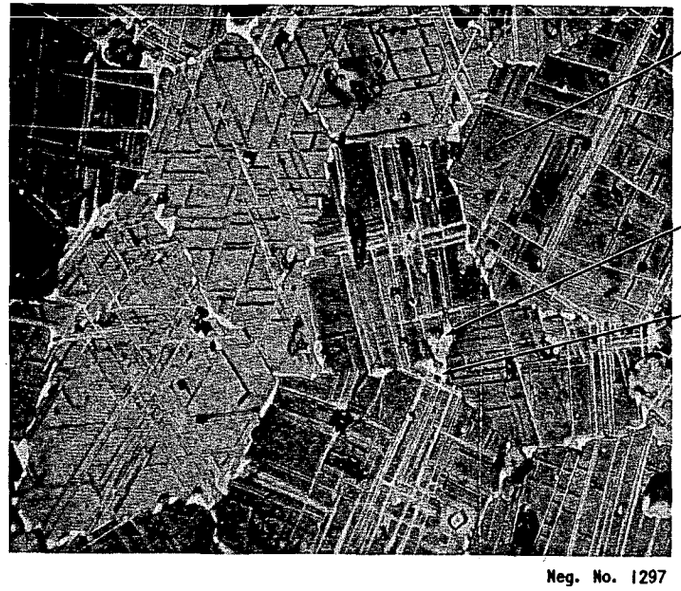

Fig. 5.2 — UC-0.1% Ni – Sintered at 1525°C, 4 hr.
Reheated at 1850°C, 1 hr in Vacuum. 500×.
Etchant: Nitric Acid-Acetic Acid-Water.

X-ray identification

Major UC
Very faint UC_2
Very faint UO_2
a_0 = 4.960 Å

experiments of (UPu)C (Section 5.3) confirmed that nickel could be evaporated by this process.

The diffusion of the nickel from the UC, together with the peritectoidal decomposition of U_2C_3 at 1780°C, are the reasons why the U_2C_3 is no longer present in the vacuum annealed sample.

The X-ray diffraction study of the samples confirmed the above results.

$(U_{0.8}Pu_{0.2})C_{0.95}$ + 0.1% Ni

Microprobe analyses were made on specimens as-sintered, and as-sintered and reheated to 1750°C in helium. The structures are shown in Section 5.3. Several standards were used: U, UC, UC + 0.1 w/o Ni, Ni, PuC, and Pu_2C_3.

The following conclusions were drawn from the results.

1. The plutonium and nickel are uniformly distributed in the monocarbide and sesquicarbide. The uniformity is better than the sensitivity of the instrument (with the possible exception of one indication, nickel is not concentrated at the grain boundaries).
2. The plutonium-to-uranium ratio in the "sesquicarbide" phase is higher than in the monocarbide phase, assuming the monocarbide phase has a Pu/U ratio of 2/8. The sesquicarbide phase would have a Pu/U ratio of 3.63/6.37.
3. Absolute plutonium and uranium analyses were hindered by surface film formations on the highly oxidizable carbides. (The samples had to be handled in air.)

5.2.2 Effect of Heat Treatment

The effects of various heat treatments on the stability of the (UPu)C structure were studied.

A. High Temperature Annealing in Helium

$(U_{0.8}Pu_{0.2})C_{0.95}$ +0.1 w/o Ni pellets were heated at 1750°C for 3 hr. The results are shown in Table 5.1 and Figs. 5.3 and 5.4.

Data obtained from the high temperature helium atmosphere annealing of $(U_{0.8}Pu_{0.2})C_{0.95}$ + 0.1 Ni are also shown in Table 5.1 and Figs. 5.3 and 5.4. The pellets lost some weight through vaporization and swelled slightly, accompanied by a density decrease. The effect is probably due to the reaction of the residual oxygen. The grain size increased, but no phase changes occurred as with UC. The annealed structure still contains sesquicarbide and no dicarbide, indicating that the decomposition temperature of the sesquicarbide is above 1750°C.

B. Vacuum Annealing Experiments

The effect of vacuum annealing on structure and composition of $(U_{0.8}Pu_{0.2})C_{0.95}$ was studied with the following objectives.

1. Reacting the Residual Oxygen (2000 to 4000 ppm) with the Carbide

   In addition to lowering the oxygen level, this could produce further densification by producing some free U and Pu which would act as a sintering aid, and then evaporate at the higher temperatures.

2. Evaporating the Nickel Sintering Aid

   Since the addition of nickel promotes the presence of the sesquicarbide phase, the removal of nickel may transform the material into a single-phase structure.

Experiments showed that the two-phase material (made with nickel sintering aid) can be converted to single-phase material by high temperature vacuum annealing.

The vacuum heating cycles used were 1900°C for 1 hr and 2200°C for 1/2 hr. To test objectives (1) and (2), materials without nickel and with 0.1 w/o nickel were

TABLE 5.1 — EFFECT OF HIGH TEMPERATURE ANNEAL ON (UPu)C + 0.1 Ni PELLETS

Experiment No.	Before Anneal				After 3 hr at 1750°C			
					Expansion, %			
	Intended Composition	Total Carbon, w/o	Sintering Temp, °C	Density, g/cm^3	Diam	Height	Density, g/cm^3	Weight Loss, %
1*	$(U_{0.8}Pu_{0.2})C_{0.95}$ + 0.1% Ni	5.25	1550	12.41	0.16	0.06	12.34	0.252
2†	$(U_{0.8}Pu_{0.2})C_{1.0}$ + 0.2% Ni	4.80	1550	12.86	0.21	0.92	12.70	0.304
3†	$(U_{0.8}Pu_{0.2})C_{1.0}$ + 0.2% Ni	4.80	1450	12.79	0.36	0.61	12.48	1.15

*Powder made from mixed oxides.
†Powder made from sesquicarbide.

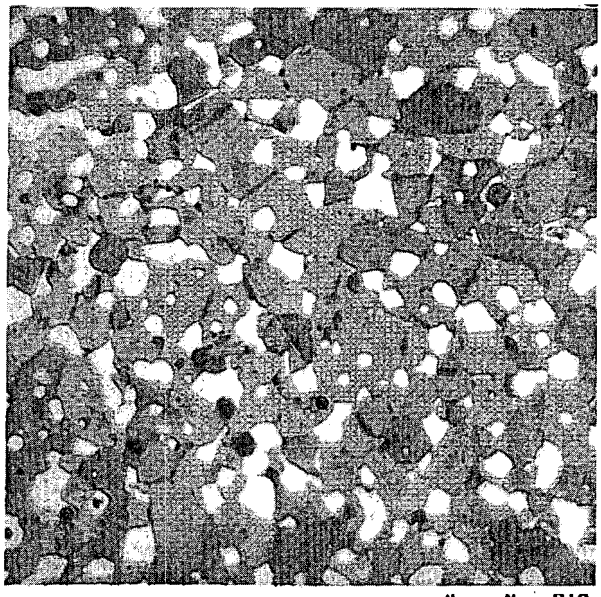

Neg. No. P12

Fig. 5.3 — $(U_{0.8}Pu_{0.2})C_{0.95}$ + 0.1% Ni – Sintered at 1550°C, 1 hr. 600×. Etchant: Nitric Acid-Acetic Acid-Water.

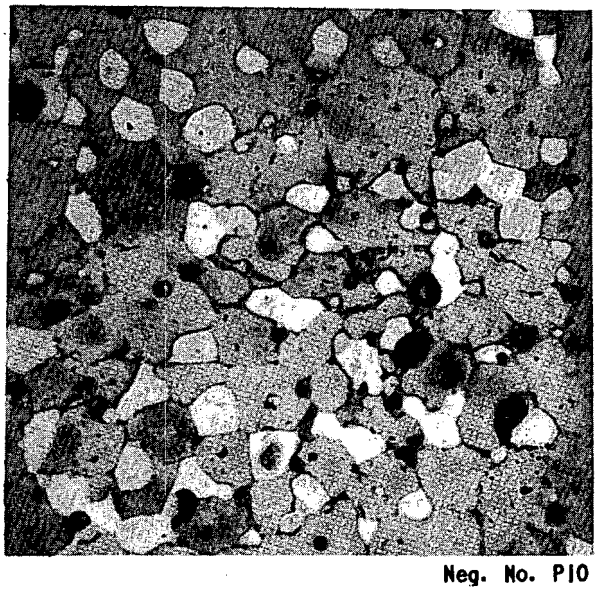

Neg. No. P10

Fig. 5.4 — $(U_{0.8}Pu_{0.2})C_{0.95}$ + 0.1% Ni – Sintered at 1550°C, 1 hr. Reheated at 1750°C, 3 hr in Helium. 600×. Etchant: Nitric Acid-Acetic Acid-Water.

run at the above conditions. The changes in dimensions, weights, and bulk densities are summarized in Table 5.2 together with the observed microstructural changes. The photomicrographs of the unannealed and annealed materials are shown in Figs. 5.5 through 5.9.

Fig. 5.5 shows the structure of a representative sample of $(U_{0.8}Pu_{0.2})C_{0.95}$ + 0.1 w/o Ni before annealing. The white areas are the sesquicarbide phase. After a 1-hr anneal at 1900°C (Fig. 5.6), the sesquicarbide phase disappeared and a grain boundary metal phase formed. Some dicarbide was also evident. When as-sintered specimens were annealed at 2200°C for 1/2 hr (Fig. 5.7), a single-phase (UPu)C structure was obtained. The grain boundary metal phase was evaporated and the excess oxygen apparently accumulated into bubbles, probably as CO, with a subsequent decrease in bulk density. The nickel content was reduced substantially by the vacuum annealing treatment, from ~1200 to ~100 ppm. Longer hold times may be necessary to reduce the oxygen content as hypothesized above.

Fig. 5.8 shows the structure of $(U_{0.8}Pu_{0.2})C_{0.95}$ before annealing. No appreciable changes in structure, weight, measurements, or density were found after annealing at 1900°C. However, after the anneal to 2200°C (Fig. 5.9), the Widmanstätten structure (dicarbide) disappeared and single-phase material was obtained. A slight density increase was obtained, perhaps indicating that some liquid-phase sintering had occurred as hypothesized in objective (1) above. The oxygen content was reduced by one-half in agreement with the hypothesis. However, further study is needed to define the mechanism of the structural changes.

5.2.3 Effect of Aging on Lattice Parameters

Studies at Harwell and Hanford have shown that the lattice parameter of plutonium compounds increases with time. The reason for the parameter increase was postulated as an alpha radiation effect.

TABLE 5.2 — EFFECT OF VACUUM ANNEALING ON $(U_{0.8}Pu_{0.2})C_{0.95}$ PELLETS PREVIOUSLY SINTERED IN HELIUM

Sintering Aid	Vacuum Treatment, ($\sim 10^{-4}$ mm Hg)	Weight Change, %	Diameter Change, in.	Bulk Density Change, %	Microstructure Change
0.1 w/o Ni	1900°C, 1 hr	-0.25	+0.0020	-3.2	Sesquicarbide phase gone. Metal grain boundary phase formed. Some "dicarbide" formed.
0.1 w/o Ni	2200°C, 1/2 hr	-1.1	-0.0033	-6.9	Single-phase material obtained. No evidence of grain boundary phase or "dicarbide" seen. Porosity is increased.
No Ni	1900°C, 1 hr	-0.09	+0.0001	-0.40	No significant change. "Dicarbide" phase still present.
No Ni	2200°C, 1/2 hr	-1.0	-0.0011	+0.77	"Dicarbide" phase gone. Single-phase material obtained.

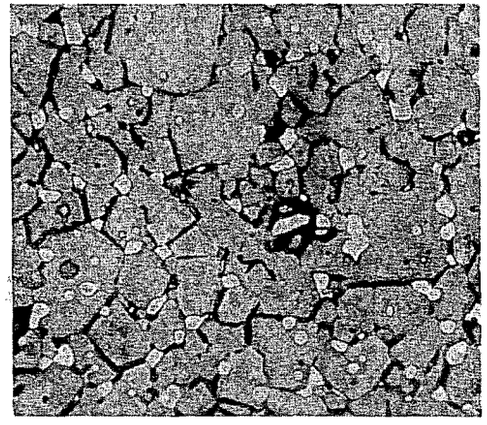

O: ~4000 ppm
Ni: ~1200 ppm
C: 4.6/4.7 w/o

Fig. 5.5 — $(U_{0.8}Pu_{0.2})C_{0.95}$ + 0.1 w/o Ni – As Sintered in Helium at 1550°C, 1/2 hr. 600×. Etchant: Nitric Acid-Acetic Acid-Water.

O: ~3600 ppm
Ni: ~140 ppm

Fig. 5.6 — $(U_{0.8}Pu_{0.2})C_{0.95}$ + 0.1 w/o Ni – Sintered in Helium and Vacuum Annealed at 1900°C, 1 hr. 600×. Etchant: Nitric Acid-Acetic Acid-Water.

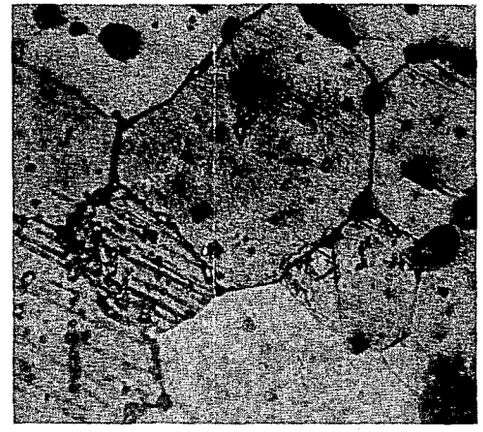

O: ~1600 ppm
Ni: ~100 ppm

Fig. 5.7 — $(U_{0.8}Pu_{0.2})C_{0.95}$ + 0.1 w/o Ni – Sintered in Helium and Vacuum Annealed at 2200°C, 1/2 hr. 600×. Etchant: Nitric Acid-Acetic Acid-Water.

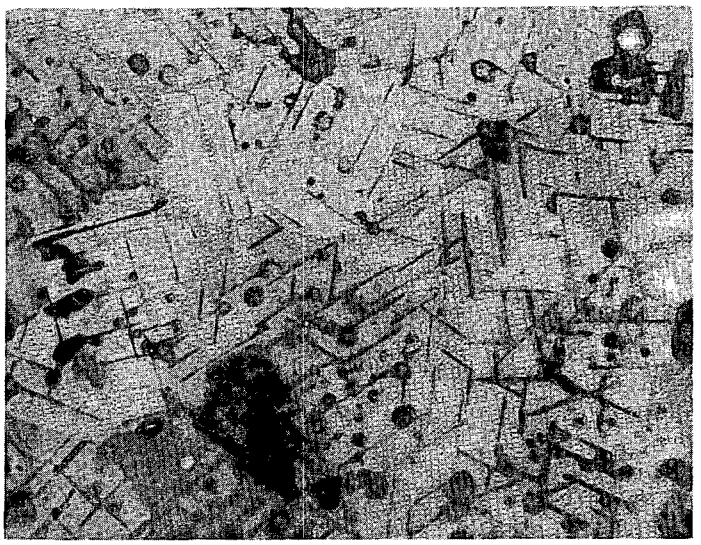

O: ~2000 ppm

Fig. 5.8 — $(U_{0.8}Pu_{0.2})C_{0.95}$ – As Sintered in Helium at 1925°C, 1 hr. 600×. Etchant: Nitric Acid-Acetic Acid-Water.

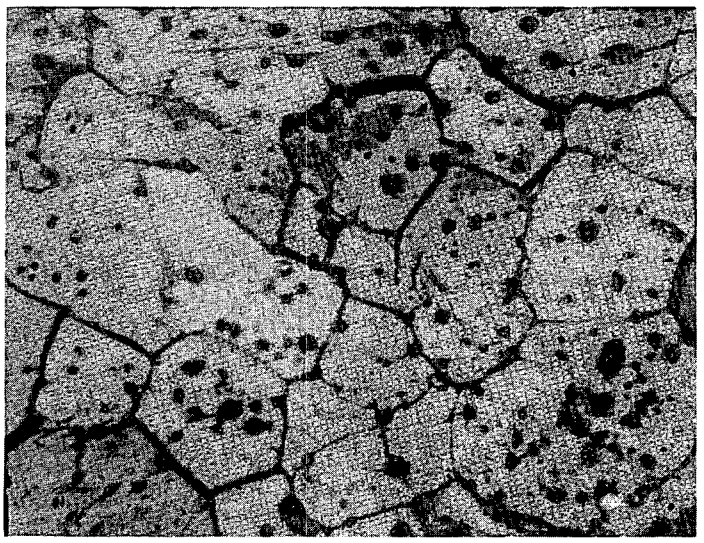

O: ~1000 ppm

Fig. 5.9 — $(U_{0.8}Pu_{0.2})C_{0.95}$ – Sintered in Helium and Vacuum Annealed at 2200°C, 1/2 hr. 600×. Etchant: Nitric Acid-Acetic Acid-Water.

A change in lattice parameter with time would be significant in the characterization of plutonium compounds; therefore, a study was initiated to determine the effect on $(U_{0.95}Pu_{0.05})C_{0.98}$ and $(U_{0.8}Pu_{0.2})C_{0.95}$. The results to date are shown in Tables 5.3 and 5.4.

A general slight increase in lattice parameter can be noted; but, considering the accuracy of the measurements, the increase is not significant within the time period studied.

5.3 $(U_{0.95}Pu_{0.05})C$ SPECIMEN FABRICATION FOR PROPERTY MEASUREMENTS

5.3.1 Powder Preparation

The program has evaluated the out-of-pile properties of mixed uranium-plutonium carbides at the 5 w/o PuC level.

A total of about 400 g of $(U_{0.95}Pu_{0.05})C_{0.98}$ powder was synthesized for the fabrication of test specimens. PuO_2, UO_2, and carbon were blended, cold-pressed without binder at about 5000 psi (pellets about 0.2 in. in diameter), and heated in helium to 1625°C with a hold time of 5½ hr. The reaction end-point was determined by monitoring the exhaust gas drawn from the heated furnace for CO.

The carbide powders were subsequently ball-milled for 24 hr in a rubber-lined mill using stainless steel balls. X-ray diffraction of the composite batches showed single-phase (UPu)C with a unit cell size, $a_0 = 4.959 \pm 0.001$ Å. The results of analyses for total carbon gave 4.79 w/o. The intended carbon content was 4.70 w/o.

5.3.2 Pellet and Other Sample Preparation

The $(U_{0.95}Pu_{0.05})C_{0.98}$ powder was used to fabricate pellets for melting point, vapor pressure, and compatibility specimens. It was also used to fabricate bars for thermal coefficient of expansion measurements.

TABLE 5.3 — EFFECT OF AGING ON LATTICE PARAMETER OF $(U_{0.95}Pu_{0.05})C_{0.98}$ POWDER (CAMERA METHOD)

Cumulative Days	Phase Present	Unit Cell Size
0	Single-phase (UPu)C	$a_0 = 4.9607 \pm 0.0003$ Å
31	Single-phase (UPu)C	$a_0 = 4.9603 \pm 0.0004$ Å
62	Single-phase (UPu)C	$a_0 = 4.9612 \pm 0.0005$ Å
90	Single-phase (UPu)C	$a_0 = 4.9613 \pm 0.0009$ Å
121	Single-phase (UPu)C	$a_0 = 4.960 \pm 0.001$ Å

TABLE 5.4 — EFFECT OF AGING ON THE LATTICE PARAMETER OF $(U_{0.8}Pu_{0.2})C_{0.95}$ POWDER (DIFFRACTOMETER METHOD)

Cumulative Days	Date	Phases Present	Unit Cell Size
0	4/15/63	Major (UPu)C Weak $(UPu)C_2$ Faint $(UPu)_2C_3$	$a_0 = 4.9648 \pm 0.0005$ Å
30	5/15/63	Major (UPu)C Faint $(UPu)_2C_3$ and $(UPu)C_2$	$a_0 = 4.9661 \pm 0.0003$ Å
69	6/23/63	Major (UPu)C Faint $(UPu)_2C_3$ and $(UPu)C_2$	$a_0 = 4.9667 \pm 0.0007$ Å
207	11/8/63	Major (UPu)C Faint $(UPu)_2C_3$ and $(UPu)C_2$	$a_0 = 4.9666 \pm 0.0004$ Å

Seventy pellets were fabricated, of which 35 contained 0.1 w/o nickel. Compacts containing nickel were prepared by blending with nickel powder in the ball mill for at least 2 hr. The powder with and without nickel was mixed with 1/4 w/o Carbowax 6000 binder and cold pressed at 30,000 psi. The size of the cold-pressed pellets was 0.224 in. in diameter by 0.215-in. high. The pellets were preheated to about 700°C in an open tantalum crucible to volatilize the binder. The final sintering was completed in a closed tantalum crucible. Pellets without the nickel sintering aid were heated to 1925°C with a hold time of 1 hr; those containing the 0.12 w/o addition of nickel were sintered at 1550°C with a hold time of 1/2 hr. Results of these experiments are shown in Table 5.5.

Metallographic examination of $(U_{0.95}Pu_{0.05})C_{0.98}$ showed structures similar to those of $(U_{0.8}Pu_{0.2})C_{0.95}$. Material without sintering aid was essentially single-phase monocarbide with some Widmanstätten dicarbide structure. Material with nickel sintering aid contained sesquicarbide in the monocarbide matrix.

Eight $(U_{0.95}Pu_{0.05})C_{0.95}$ coefficient of expansion bars, 2.230-in. long, 0.233-in. wide, and 0.340-in. high were fabricated (four with nickel sintering aid and four without).

The bars were cold pressed at 13,000 psi (maximum pressure attainable with the existing pressing equipment) and contained the usual 1/4 w/o Carbowax binder. The bars, with and without the nickel additions, subsequently were sintered for 1 hr at 1550 and 1925°C, respectively. The bars containing the nickel addition met size and camber specifications after the sintering operation, and grinding was unnecessary. However, those without the nickel addition were warped excessively, and had to be reheated and ground. Results of these experiments are shown in Table 5.6.

TABLE 5.5 — RESULTS OF SINTERING EXPERIMENTS WITH $(U_{0.95}Pu_{0.05})C_{0.98}$ PELLETS
[Pellet Density, g/cm^3 (10 Pellets)]

Experiment No.	Sintering Conditions	Intended Composition	Range	Average	Plutonium,* w/o	Total Carbon,† w/o	Nitrogen, ppm	X-Ray Analysis
1	1925°C, 1 hr	$(U_{0.95}Pu_{0.05})C_{0.98}$	12.24 to 13.37	12.31	4.9	4.67	273	Single-phase (UPu)C $a_0 = 4.9616 \pm 0.0003$ Å
2	1550°C, 1/2 hr	$(U_{0.95}Pu_{0.05})C_{0.98}$ plus 0.1 w/o Ni	12.93 to 13.15	13.04	4.6	4.79	144	Single-phase (UPu)C $a_0 = 4.961 \pm 0.001$ Å

*Intended plutonium content: 4.75%.
†Intended carbon content: 4.70 w/o.

TABLE 5.6 — RESULTS OF SINTERING EXPERIMENTS WITH $(U_{0.95}Pu_{0.05})C_{0.98}$ BARS
(BARS FOR THERMAL EXPANSION STUDIES)

Intended Composition	Sintering Temp, °C	Hold Time, hr	Bar Density, g/cm^3 (Two Bars)	Plutonium,* w/o	Total Carbon,† w/o	Nitrogen, ppm	X-Ray Analysis
$(U_{0.95}Pu_{0.05})C_{0.98}$	1925	1	11.80-11.81	4.6	4.67	251	Single-phase (UPu)C $a_0 = 4.9607 \pm 0.0003$ Å
$(U_{0.95}Pu_{0.05})C_{0.98}$ plus 0.12 w/o Ni	1550	1	13.17-13.29	5.1	4.77	272	Single-phase (UPu)C $a_0 = 4.962 \pm 0.001$ Å

*Intended plutonium content: 4.75%.
†Intended carbon content: 4.70 w/o.

5.4 FUEL-CLAD COMPATIBILITY

5.4.1 Introduction

The compatibility of UC and $(U_{0.95}Pu_{0.05})C_{0.98}$ with potential cladding materials was studied under conditions similar to those that would prevail in a fuel element: 590°C (1100°F) and 820°C (1500°F) for 1000 to 4000 hr. Metallographic examination, subsequent to the tests, determined the degree of interaction between fuel and cladding samples. The results with (UPu)C were similar to those obtained earlier with UC. These data are summarized in Tables 5.7 and 5.8. There were no significant reactions between fuel and stainless steel, $2\frac{1}{4}$ Cr-1 Mo steel, niobium and niobium-1% zirconium alloy. Significant reactions were noted with Zircaloy-2, Inconel-X, and beryllium.

All the fuel samples had a hyperstoichiometric structure, that is, a monocarbide matrix with a second-phase of higher carbides. The carbon content was hypostoichiometric, but the carbide had sufficient oxygen in solid solution to produce a hyperstoichiometric "equivalent carbon" content.

Fuel and cladding materials were held in contact with each other in capsules similar to the one shown in Fig. 5.10. Continued contact between fuel and cladding samples at elevated temperatures was assured by the greater thermal expansion of the stainless steel insert compared to the Inconel container. Most of the capsules contained duplicates of the same cladding materials. The capsules were seal-welded in a glove box containing a helium atmosphere, decontaminated, leak-checked, taken out of the glove box line, and placed in the sealed inner shell of the furnaces. The furnaces stood in a hood in the plutonium facility.

5.4.2 Tests with UC

A. Type 304 Stainless Steel (Tested 1000, 2000, and 4000 hr at 820°C)

No significant reactions were noted at any of the test durations. A typical inter-

TABLE 5.7 — UC COMPATIBILITY TEST RESULTS*

Material	Temp, °C (°F)	Results by Metallographic Examination		
		1000-hr Tests	2000-hr Tests	4000-hr Tests
Type 304	820 (1500)	No reaction	No reaction	No reaction
$2\frac{1}{4}$ Cr-1 Mo	820 (1500)	—	—	No reaction
Nb	820 (1500)	No reaction	No reaction	No reaction
Zircaloy-2	820 (1500)	—	—	Reaction noted
Be	820 (1500)	—	—	Reaction noted
Inconel-X	820 (1500)	Reaction noted	Reaction noted	Reaction noted

*Tests conducted in helium in differential expansion capsule.

TABLE 5.8 — (UPu)C COMPATIBILITY TEST RESULTS*

Material	Temp, °C (°F)	Results by Metallographic Examination	
		1000-hr Tests	4000-hr Tests
Type 316 vs $(U_{0.95}Pu_{0.05})C_{0.98}$	590 (1100)	—	No reaction
	820 (1500)	No reaction	No reaction
Type 316 vs $(U_{0.95}Pu_{0.05})C_{0.98}$ + 0.1 Ni	590 (1100)	—	No reaction
	820 (1500)	No reaction	No reaction
$2\frac{1}{4}$ Cr-1 Mo vs $(U_{0.95}Pu_{0.05})C_{0.98}$	590 (1100)	—	No reaction
	820 (1500)	—	No reaction
Nb, Nb-1 Zr vs $(U_{0.95}Pu_{0.05})C_{0.98}$	590 (1100)	—	No reaction
	820 (1500)	No reaction	No reaction†
Nb, Nb-1Zr vs $(U_{0.95}Pu_{0.05})C_{0.98}$ + 0.1 Ni	590 (1100)	—	No reaction
	820 (1500)	No reaction	No reaction
Zircaloy-2 vs $(U_{0.95}Pu_{0.05})C_{0.98}$	590 (1100)	Reaction noted	—
	820 (1500)	Reaction noted	—

*Tests conducted in helium in differential expansion capsule.
†One sample showed a possible reaction to a depth of 0.0002 in. maximum.

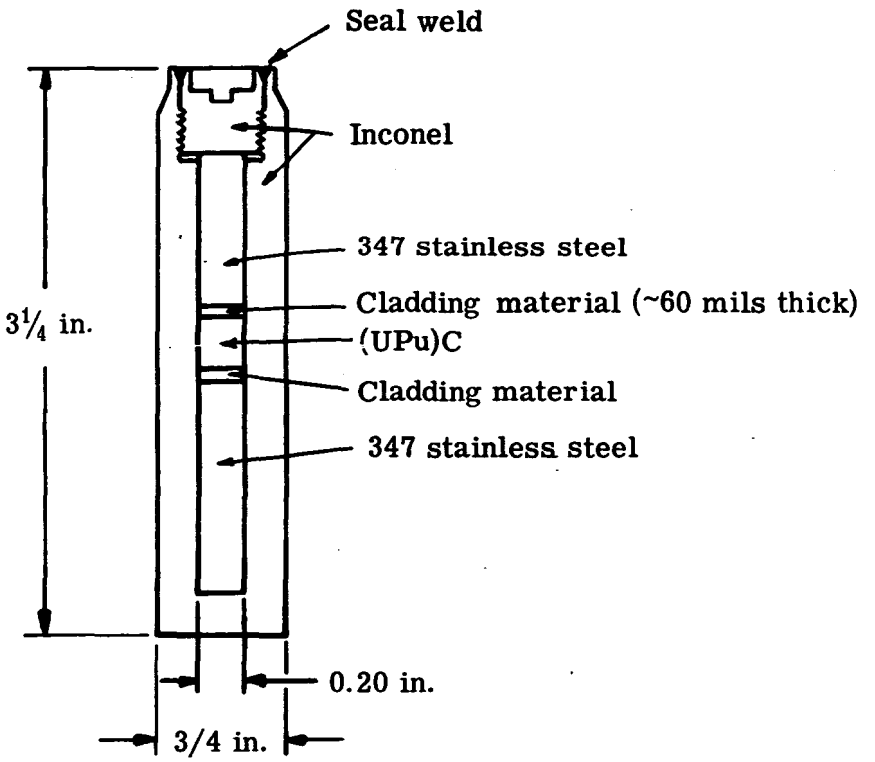

Fig. 5.10 — Compatibility Capsule

face is shown in Fig. 5.11. Slight local interactions (<1-mil penetration) were seen, but they could not be identified either by metallography, X-ray diffraction, or microprobe analysis.

Microprobe analysis of the specimen tested for 2000 hr showed there was no uranium penetration. An inclusion, such as shown on Fig. 5.11, was 75% uranium with no iron, chromium, or nickel. These inclusions are probably adhering UC which had oxidized to U_3O_8 (75 to 76% uranium) on storage.

B. 2¼ Cr-1 Mo Alloy Steel (Tested 4000 hr at 820°C)

No significant reactions were noted. A typical interface is shown in Fig. 5.12.

Microprobe analysis of the 2¼ Cr-1 Mo specimen tested for 4000 hr showed no uranium penetration. The nonmetallic phase on the surface of 2¼ Cr-1 Mo photomicrograph (Fig. 5.12) had a high uranium content. The material is probably oxidized UC which adhered to the surface of the steel.

C. Inconel-X (Tested 1000, 2000, and 4000 hr at 820°C)

A considerable reaction occurred between UC and fully aged Inconel-X at all three test durations. Typical interfaces are shown in Figs. 5.13 and 5.14.

A metallic appearing diffusion zone was formed between UC and Inconel-X; however, the specimens did not adhere to each other on disassembly of the capsule. The Inconel-X surface was penetrated by voids; the shape of the voids indicated that melting probably occurred. The penetration of voids into the Inconel-X surface and the thickness of the metallic diffusion layer on the UC were measured and are presented in Table 5.9.

Microprobe analysis of the Inconel-X sample which had been tested for 1000 hr did not reveal uranium penetration outside the voids formed by the Ni-U eutectic (Fig. 5.14). The white areas adjacent to the voids were identified as Cr_7C_3 by a

TABLE 5.9 — INCONEL-X – UC INTERACTION

Test Duration, hr	Penetration of Voids into Inconel-X, mils		Diffusion Layer Thickness on UC, mils
	Max	Avg	Avg
1000	2.8	2	1.0
2000	3.1	3	1.7
4000	4.8	4	2.5

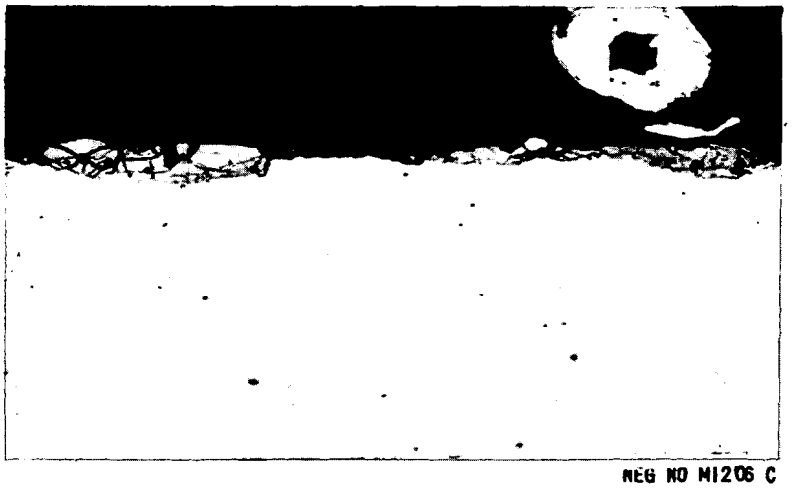

Fig. 5.11 — Type 304 SS Tested 1000 hr – 500× – Unetched

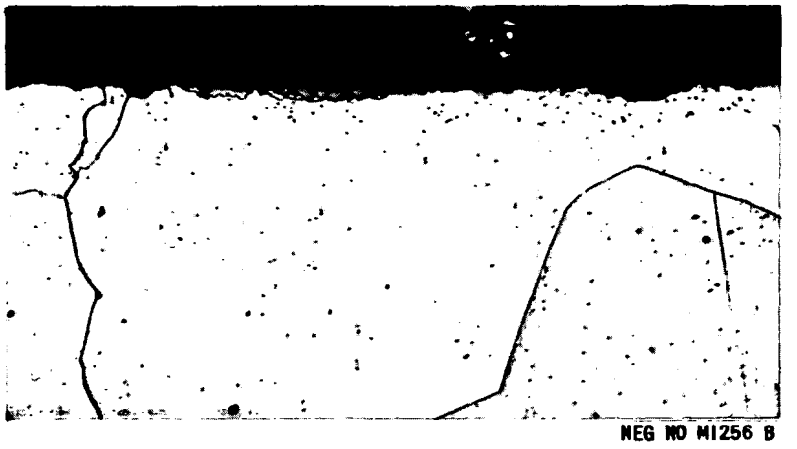

Fig. 5.12 — $2\frac{1}{4}$ Cr-1 Mo Steel Tested 4000 hr – 500× – Nital Etch

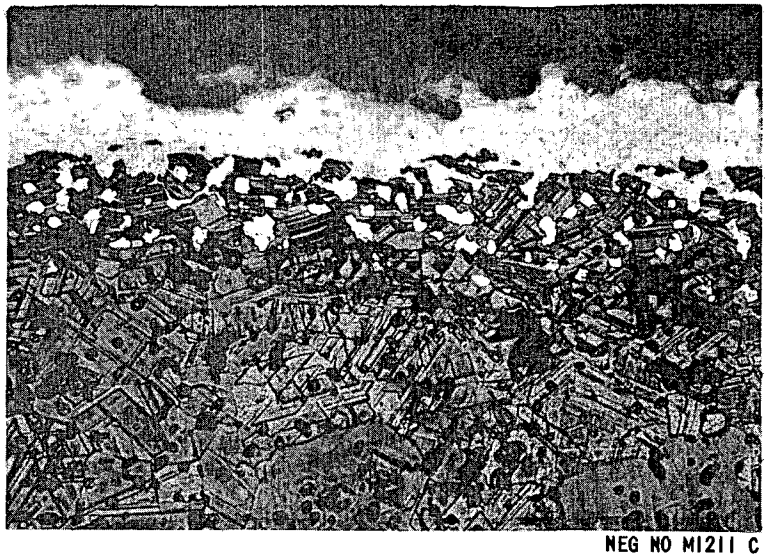

Fig 5.13 — UC Tested 1000 hr in Contact with Inconel-X – 500× – Nitric Acid-Acetic Acid-Water Etch

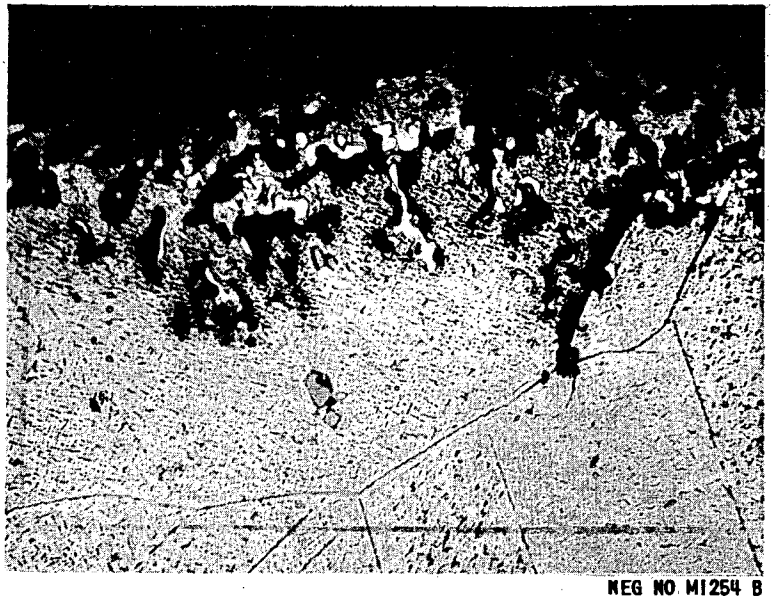

Fig. 5.14 — Inconel-X, Tested 4000 hr – 500× – Aqua Regia Etch

combination of microprobe and X-ray diffraction analysis. The metallic diffusion layer on the UC half of the interface (Fig. 5.13) was identified as uranium-nickel binary carbides of the M_3C and M_7C_3 types. Microprobe analysis showed the composition to be about half nickel, half uranium. The nickel concentration increased toward the Inconel-X interface. The nickel penetrated the UC to a 15 μ depth. The nickel concentration in the UC was up to a maximum of 1.5%. The above data indicate that a U-Ni-C phase was formed at the test temperature. Upon cooling, UC with a small amount of nickel was precipitated out of the U-Ni-C solution at the UC interface. At the Inconel-X interface the Ni-U eutectic was formed, and on cooling, some of the excess carbon formed chromium carbides. The diffusion zone in between formed the binary uranium-nickel carbides. X-ray diffraction analysis of the interface did not reveal any U_XNi_y compounds. Compacts made subsequently, containing up to 5 w/o Ni, did not show any U_XNi_y compounds either. This is contrary to the findings of some other investigators who have identified U-Ni compounds as reaction products.

D. Niobium (Tested 1000, 2000, and 4000 hr at 820°C)

The niobium samples did not show any metallographic evidence of interaction with UC in any of the tests. A typical interface is shown in Fig. 5.15. X-ray diffraction of the interface after the 4000 hr test showed some hexagonal Nb_2C lines. Since the niobium carbide was undetectable by metallography, the layer must be very thin.

Microhardness readings were made to check the extent of carburization of the niobium, since carburization would cause embrittlement of the niobium. The niobium sheet, as received, had a 125 Vickers hardness (50-g load) near the edge. The niobium sheet which had been in contact with UC for 4000 hr had an 85 Vickers hardness near the edge. Some annealing, and no measurable embrittlement, had occurred.

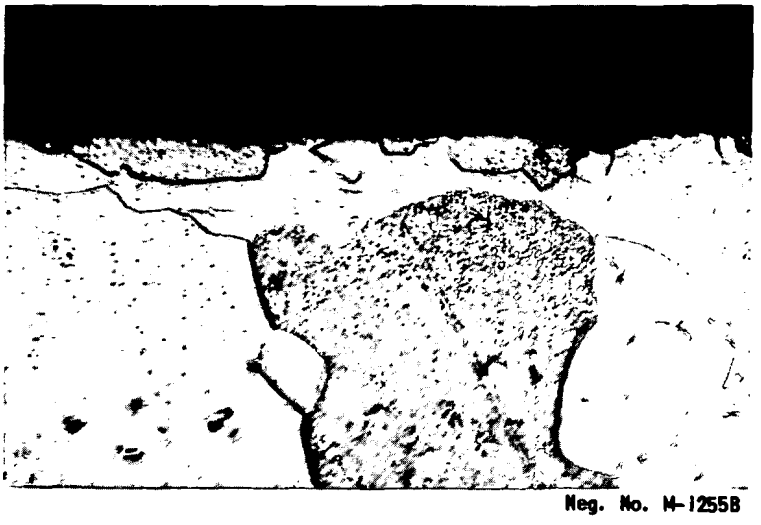

Fig. 5.15 — Niobium Tested 4000 hr – 500×.
Etched in 1% KBr, 1% NH_4Cl, 3% NaF in
1N H_2SO_4.

E. Zircaloy-2 (Tested 4000 hr at 820°C)

The Zircaloy reacted with the UC. Visual as well as metallographic examination showed that melting had occurred. The cause of the melting was probably the formation of a eutectic between the Zircaloy and the container materials during an accidental 8-hr overheat to 980°C. The Fe-Zr eutectic is at 934°C and the Ni-Zr eutectic is at 961°C.

The interface was bonded in a number of locations. Microhardness measurements were made. These are shown together with the microstructure in Fig. 5.16. Microhardness, X-ray diffraction, in combination with microprobe analyses performed by other investigators show that ZrC and free uranium metal are formed.

F. Beryllium (Tested 4000 hr at 820°C)

A considerable reaction occurred with UC. A molten metallic phase was observed visually. Metallographic examination of the beryllium specimen under polarized light indicated the material was no longer beryllium metal. X-ray diffraction indicated it had been converted to UBe_{13}. The sample had been tested for 4000 hr. The UC-UBe_{13} interface is shown in Fig. 5.17.

5.4.3 Tests with $(U_{0.95}Pu_{0.05})C_{0.98}$

The fuel samples used are described in Section 5.3. All the samples were hypostoichiometric in carbon content, but had sufficient oxygen in solid solution to produce microstructures with higher carbides and no free metal.

A. Type 316 Stainless Steel

There were no reactions between fuel and type 316 stainless steel samples. Typical samples of steel which had been in contact with fuel are shown in Fig. 5.18. The carbide and sigma precipitation in the steel are a thermal effect, and are not a product of interaction with the fuel.

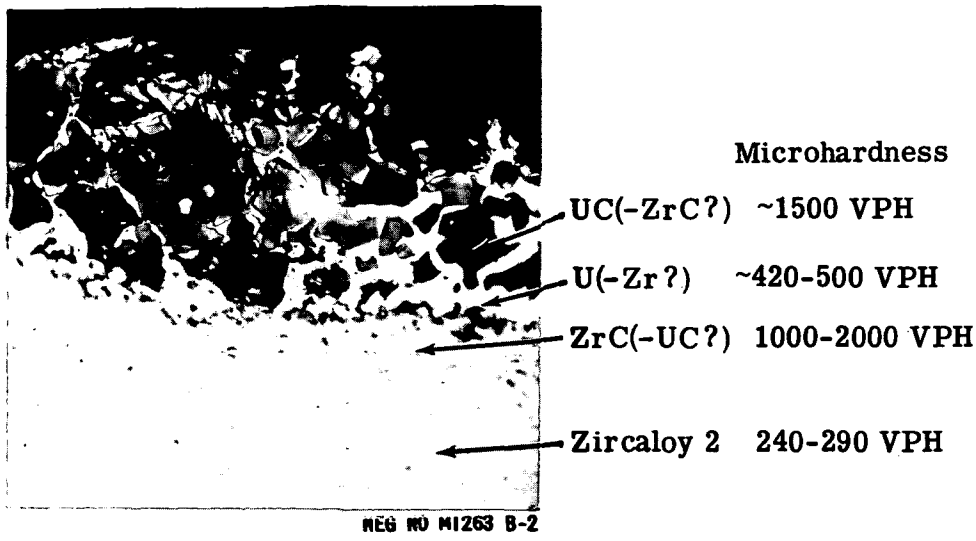

Fig. 5.16 — Zircaloy-2-UC Interface Tested 4000 hr at 820°C – 500×

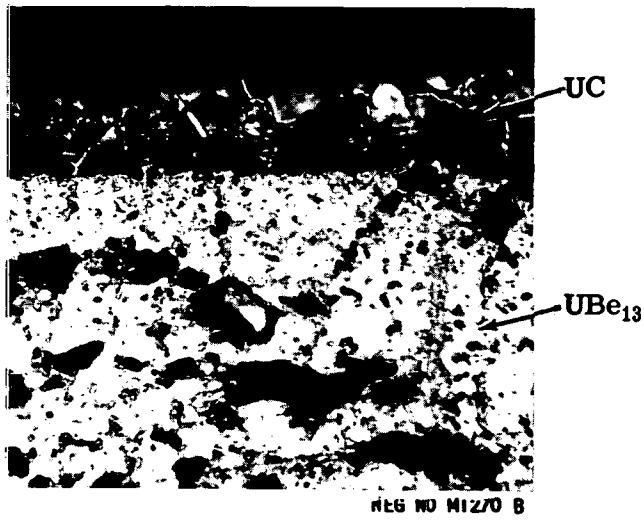

Fig. 5.17 — Beryllium-UC Interface Tested 4000 hr at 820°C – 500×

Glyceregia etch 150×

From test with $(U_{0.95}Pu_{0.05})C_{0.98}$ for 4000 hr at 593°C (1100°F)

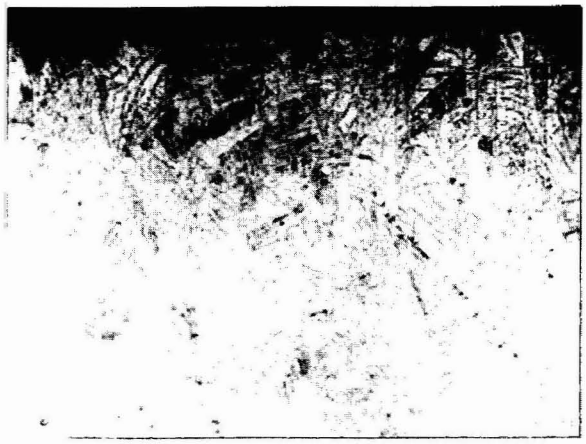

Glyceregia etch 100×

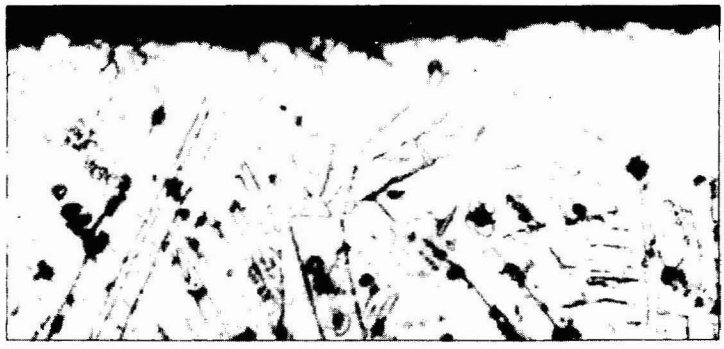

Glyceregia etch 600×

From test with $(U_{0.95}Pu_{0.05})C_{0.98}$ for 4000 hr at 816°C (1500°F)

Fig. 5.18 — Type 316 Stainless Steel from Compatibility Test

B. $2\frac{1}{4}$ Cr-1 Mo Steel

There were no reactions between fuel and $2\frac{1}{4}$ Cr-1 Mo steel.

A typical sample of steel which had been in contact with fuel is shown in Fig. 5.19. Considerable grain growth occurred at the higher test temperature, as would be expected.

C. Niobium, Niobium-1 w/o Zirconium

There were no reactions between fuel and niobium, or niobium-1 w/o zirconium alloy with the exception of one case. A typical niobium sample which was in contact with fuel and did not react is shown in Fig. 5.20. Typical niobium-1 w/o zirconium samples that were in contact with the fuel are shown in Fig. 5.21. One of the samples reacted slightly with the fuel. The reaction layer is an average of 0.008 mm (0.0003 in.) thick. Its composition was not identified although a reaction between UC and Zr or ZrO_2 is suspected. The niobium was annealed by the test temperature, whereas the niobium-1 w/o zirconium was not.

D. Zircaloy-2

A reaction was noted between $(U_{0.8}Pu_{0.2})C_{0.95}$ and Zircaloy-2. Fig. 5.22 shows a typical Zircaloy-2 interface with the fuel. The reaction product was not identified.

5.5 COEFFICIENT OF THERMAL EXPANSION MEASUREMENTS

The coefficient of thermal expansion was determined from room temperature to 1400°C in vacuum for sintered $(U_{0.95}Pu_{0.05})C_{0.98}$ with and without nickel sintering aid. The presence of the sintering aid did not affect the coefficient of expansion significantly. The values obtained for the mixed uranium-plutonium carbides are about 5% higher than the literature values given for UC. The results of this investigation are in general agreement with those of other investigators. The comparison is made in Table 5.10.

TABLE 5.10 — SUMMARY OF CARBIDE THERMAL EXPANSION COEFFICIENTS

Material	Source	Temperature Range, °C	Coefficient, 10^{-6}/°C	Reference
Sintered UC	Taylor (Carborundum Co.)	25-950	11.2	23
Sintered UC	Crane (United Nuclear)	25-950	11.4	24
Cast UC	Crane (United Nuclear)	25-950	11.6	24
Cast UC	Secrest (BMI)	25-950	11.4	25
Cast $(U_{0.87}Pu_{0.13})C$	Ogard (LA)	25-900	11.1	26
Cast $(U_{0.85}Pu_{0.15})C$	(Harwell)	25-1000	11.1-11.8	27
Sintered $(U_{0.85}Pu_{0.15})C$	(Harwell)	25-1000	11.1	27
Hot pressed $(U_{0.85}Pu_{0.15})C$	(Harwell)	25-1000	10.8	27
Sintered $(U_{0.8}Pu_{0.2})C_{0.95}$	Stahl (United Nuclear)	25-950	11.3	22
		25-1400	11.9	22
Sintered $(U_{0.8}Pu_{0.2})C_{0.95}$ + 0.1 w/o Ni	Stahl (United Nuclear)	25-950	11.4	22
		25-1400	12.3	
Sintered $(U_{0.95}Pu_{0.05})C_{0.98}$	Stahl (United Nuclear)	25-1000	12.0	This report
		25-1400	12.6	This report
Sintered $(U_{0.95}Pu_{0.05})C_{0.98}$+ 0.1 w/o Ni	Stahl (United Nuclear)	25-1000	11.8	This report
		25-1400	12.2	This report

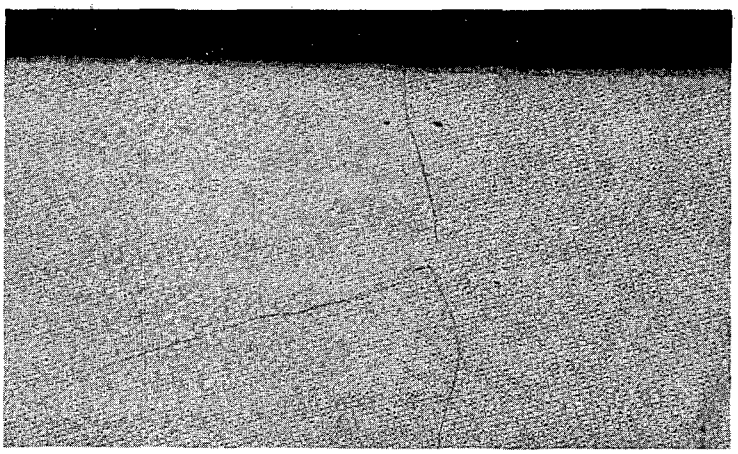

Nital etch 150×

From test with $(U_{0.95}Pu_{0.05})C_{0.98}$ for 4000 hr at 816°C (1500°F)

Fig. 5.19 — $2\frac{1}{4}$ Cr-1 Mo Steel from Compatibility Test

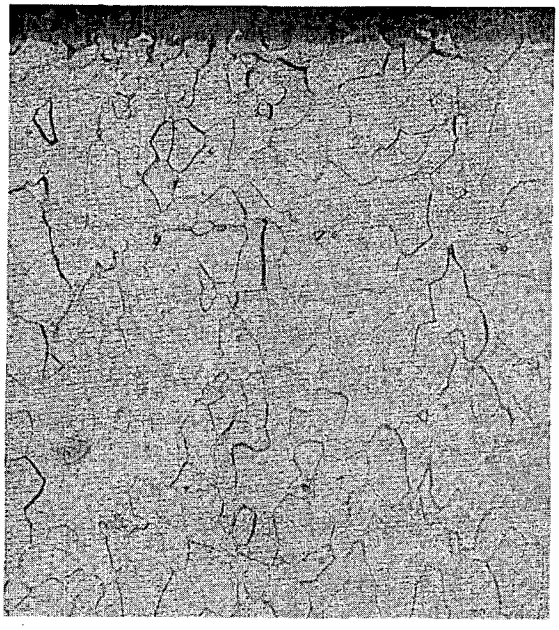

150 ×

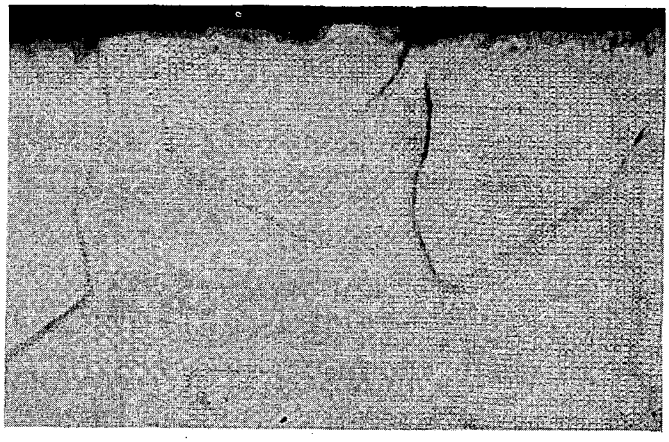

600 ×

From test with $(U_{0.95}Pu_{0.05})C_{0.98}$ for 4000 hr at 816°C (1500°F)

Fig. 5.20 — Niobium from Compatibility Test

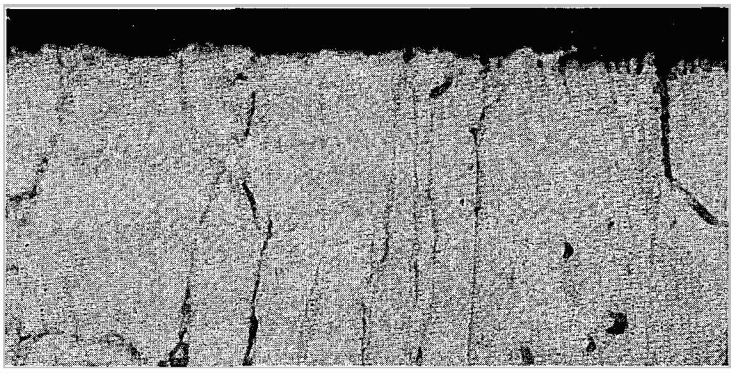

600×

From test with $(U_{0.95}Pu_{0.05})C_{0.98}$ + 0.1 w/o Ni for 4000 hr at 816°C (1500°F)

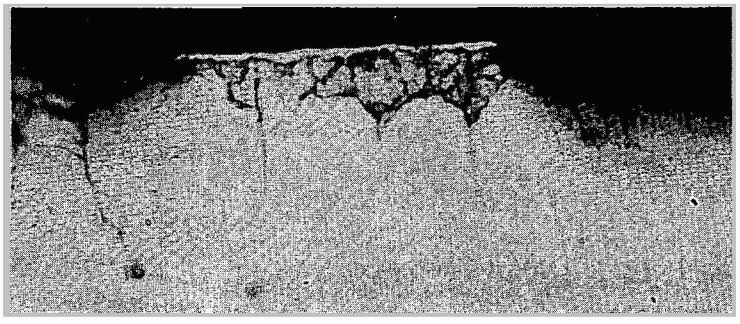

600×

From test with $(U_{0.95}Pu_{0.05})C_{0.98}$ for 4000 hr at 816°C (1500°F). Reaction layer is 0.0003 in., average.

Fig. 5.21 — Niobium-1% Zirconium from Compatibility Test

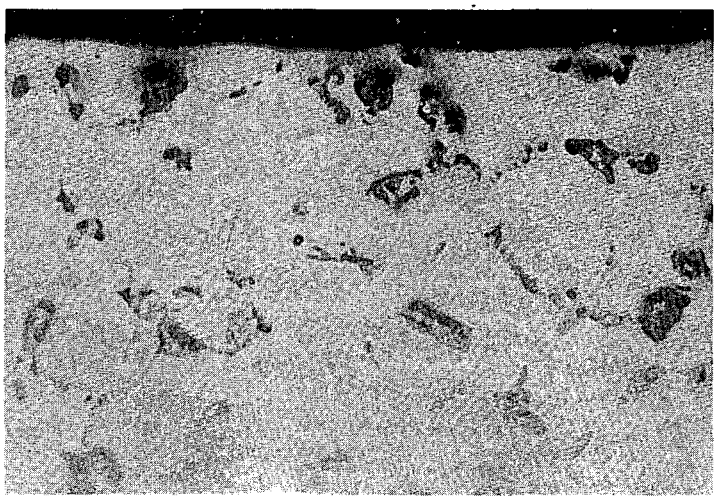

150×

From test with $(U_{0.95}Pu_{0.05})C_{0.98}$ for 1000 hr at 816°C (1500°F)

Fig. 5.22 — Zircaloy-2 from Compatibility Test

The detailed data for $(U_{0.95}Pu_{0.05})C_{0.98}$ are given in Tables 5.11 and 5.12 and include the results of two heating and cooling runs for each specimen. The accuracy of the values is about ±5%. The expansion curves were smooth, and did not show any transformation.

Prior to the testing of carbides, a tantalum standard was tested in vacuum, to 1485°C, to obtain a calibration curve for the alumina dilatometer. The curve obtained for alumina checked those of previous investigators within ±7%. The spread of values for alumina among previous investigators is ±3%.

The coefficients were determined with a differential dilatometer consisting of high purity, high density, tubular alumina elements shown schematically in Fig. 5.23. The difference in expansion between the alumina and the specimen was sensed by both a dial gauge and a linear transformer. The nominal specimen size was 0.2 in. by 0.3 in. by 0.2-in. long. No appreciable changes in dimensions were found after testing of the specimens. In addition, no appreciable changes in structure or composition of the test specimens were noted.

5.6 MELTING POINT DETERMINATIONS

The melting point (liquidus temperature) of $(U_{0.95}Pu_{0.05})C_{0.98}$ was determined as 2535 ± 20°C. The solidus is estimated to be 2500 ± 20°C, based on one experiment. The melting point data are given in Table 5.13. All specimens contained about 2000 ppm of oxygen as-fabricated.

The above data are bracketed by the melting point of $(U_{0.8}Pu_{0.2})C_{0.95}$ obtained previously by United Nuclear, and by the melting point of UC obtained by Los Alamos (Table 5.13). They are in line with the trend of decrease in melting point with increasing plutonium content.

The specimens (cylinders about 0.2-in. diameter and 0.2-in. long) were heated in a tantalum resistance vacuum furnace in internally carburized tantalum cups.

TABLE 5.11 — COEFFICIENT OF EXPANSION OF $(U_{0.95}Pu_{0.05})C_{0.98}$

Temperature Range, °C	Thermal Expansion Coefficients, 10^{-6}/°C						
	Transformer			Dial Gauge			Over-All Value (all runs)
	First Heating	First Cooling	Second Heating	First Heating	First Cooling	Second Heating	
25-200	9.42	8.58	8.29	8.68	9.70	9.42	9.0
25-400	10.4	9.20	9.75	10.7	10.7	10.0	10.0
25-600	11.1	11.5	10.3	10.6	11.7	10.8	10.8
25-800	11.7	12.1	11.2	11.4	12.4	11.6	11.6
25-1000	12.2	12.5	11.8	11.7	12.8	12.1	12.0
25-1200	12.7	12.7	12.2*	12.2	13.0	12.4*	12.4
25-1400	13.1	12.9	12.4	12.5	13.3	12.6	12.6

*Interpolated.

TABLE 5.12 — COEFFICIENT OF EXPANSION OF $(U_{0.95}Pu_{0.05})C_{0.98}$ + 0.1 w/o Ni

Temperature Range, °C	Thermal Expansion Coefficients, 10^{-6}/°C						
	Transformer			Dial Gauge			Over-All Value (all runs)
	First Heating	First Cooling	Second Heating	First Heating	First Cooling	Second Heating	
25-200	8.58	7.55	8.87	9.15	9.71	8.30	8.60
25-400	10.9	8.75	9.86	10.2	10.7	9.20	10.2
25-600	11.7	9.73	10.8	10.8	11.7	10.1	10.9
25-800	12.0	10.7	11.3	11.4	12.3	10.8	11.4
25-1000	12.2	11.7	11.7	12.0	12.9	11.3	11.8
25-1200	12.2	12.4	11.9	12.1	13.4	11.6	12.1
25-1400	12.2	12.5	12.1	12.2	13.4	11.7	12.2

TABLE 5.13 — (UPu)C MELTING POINT DATA

Material	Run No.	Corrected Liquidus Temp, °C	Corrected Solidus Temp, °C	Reference
$(U_{0.95}Pu_{0.05})C_{0.98}$ (impurities: 2000 ppm O, 200 ppm N)	1	—	2500 ± 20	This report
	2	2535 ± 20	—	This report
	3	2540 ± 20	—	This report
	4	2530 ± 20	—	This report
$(U_{0.8}Pu_{0.2})C_{0.95}$ (impurities: 2000 ppm O, 200 ppm N)	UNC	2480 ± 20	2430 ± 20	22
UC	LASL	2560 ± 50	—	12

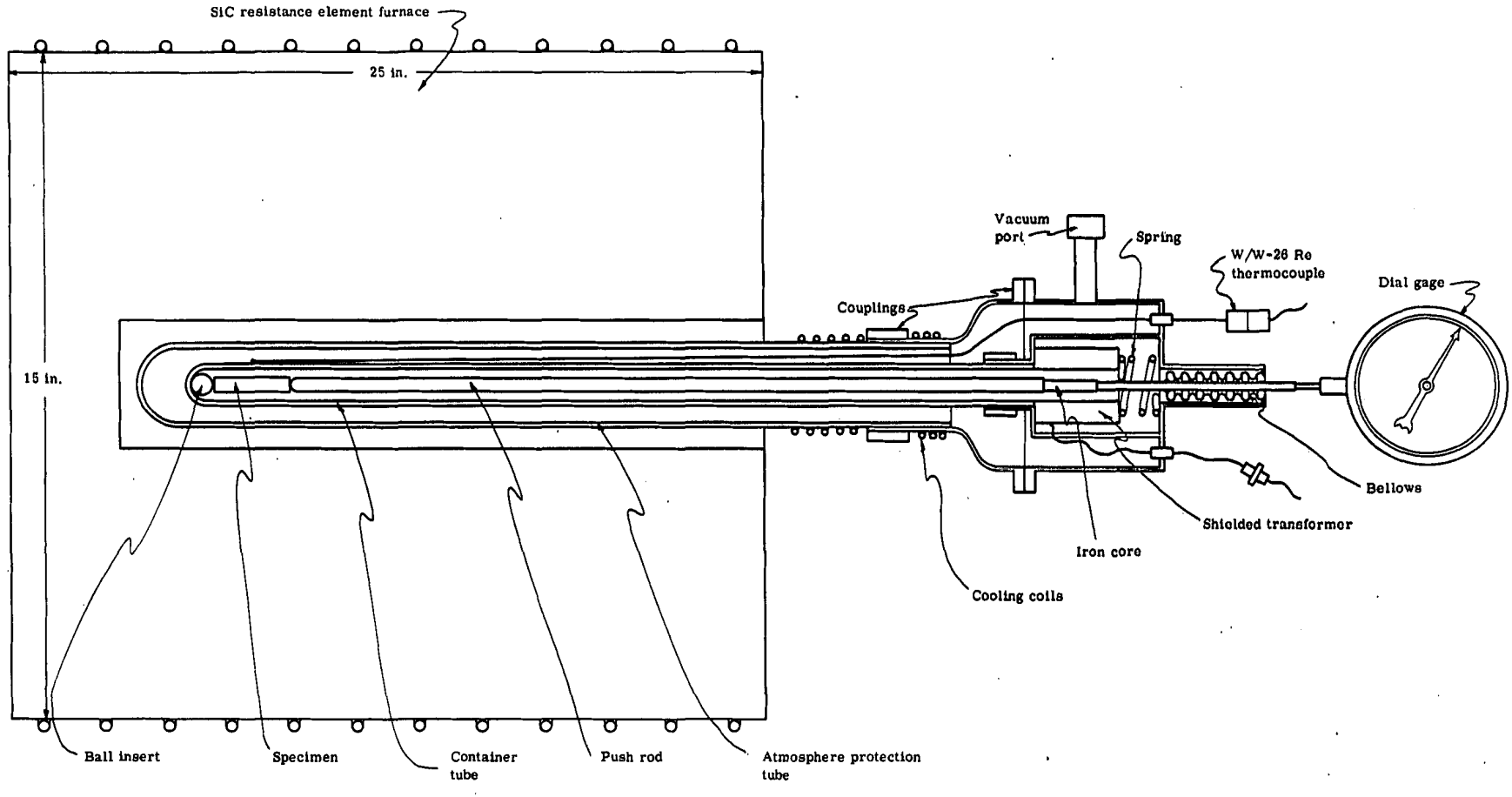

Fig. 5.23 — Schematic of Dilatometer

Temperature was measured optically with a Pyro Micro-Optical pyrometer by sighting directly on the specimen. Standards of pure (99.9+) copper, titanium, alumina, and niobium were melted to establish the correction curve for sight glass and glove box window absorption errors.

5.7 THERMAL STABILITY AND VAPOR PRESSURE MEASUREMENTS

5.7.1 Introduction

Thermal stability and vapor pressure of $(U_{0.95}Pu_{0.05})C_{0.98}$ were determined by the Knudsen effusion technique. The vapor pressures of uranium and plutonium over $(U_{0.95}Pu_{0.05})C_{0.98}$ are summarized below:

°C	°K	Uranium, atm	Plutonium, atm
1822	2095	9×10^{-8}	1 to 2×10^{-6}
1995	2270	3×10^{-6}	1 to 2×10^{-5}

The plutonium vaporized faster than uranium, but the percentage carbon content, and hence the structure, did not change appreciably. The uranium vapor pressure over (UPu)C was very similar to that of uranium over UC at 2000°C, i.e., 2×10^{-6} atm.

5.7.2 Experimental Equipment

The Knudsen effusion method was used with the apparatus shown schematically in Fig. 5.24.

The Knudsen effusion cell was 3/8-in. diameter by 5/8-in. high and was formed from a spun tantalum cup and cover, and was welded. The cover of the cell contained a 0.030- to 0.040-in. diameter orifice in a stepped down portion ~0.0015-in. thick. The cell was internally carburized prior to assembly to prevent fuel-tantalum reactions. The high orifice diameter-to-depth ratio was to reduce channeling effects.

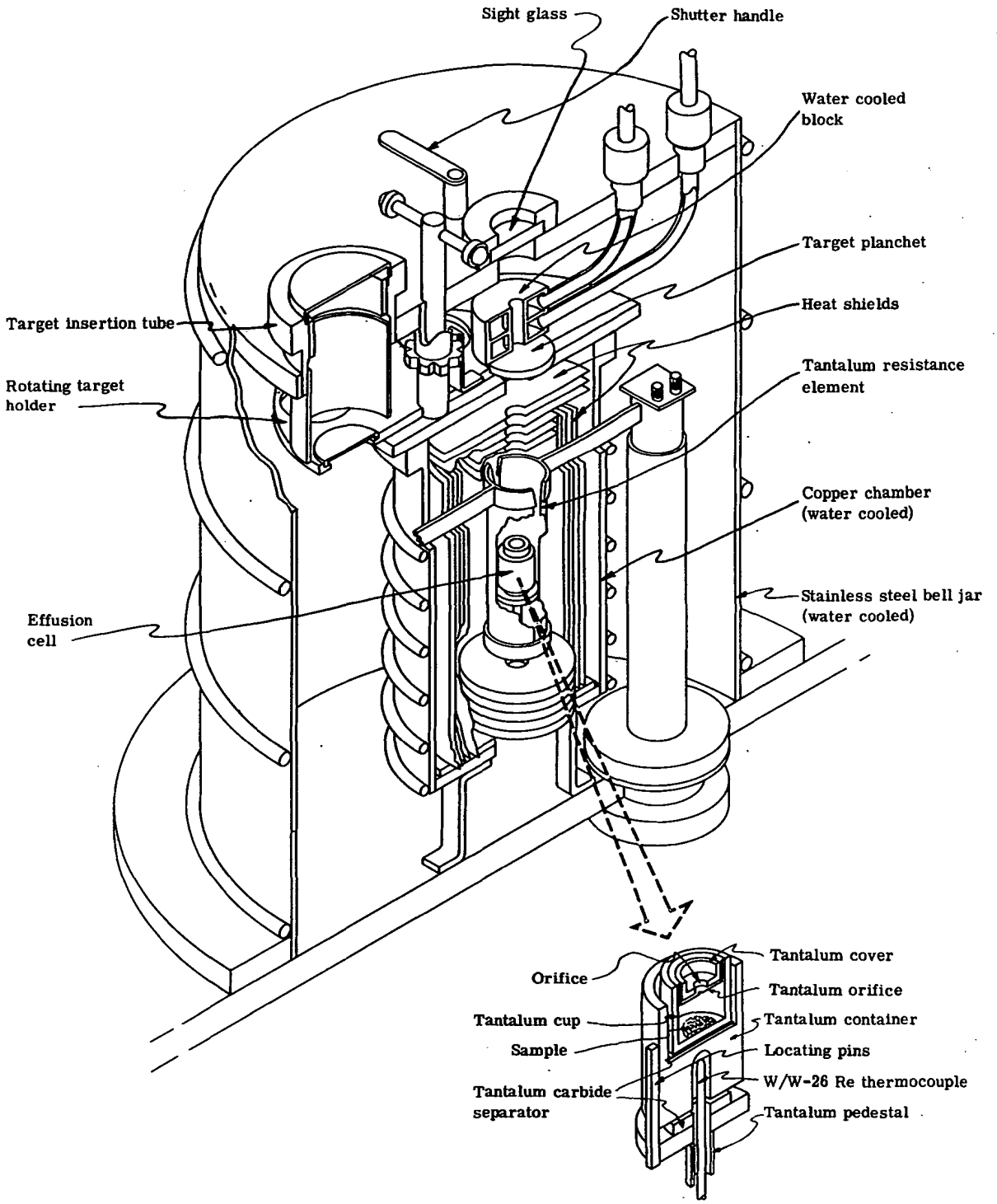

Fig. 5.24 — Schematic of Knudsen Vapor Pressure Apparatus

5.7.3 Experimental Data

Knudsen cells with electropolished and subsequently crushed $(U_{0.95}Pu_{0.05})C_{0.98}$ were tested at 1822 and 1995°C at an average background pressure of 4 to 6×10^{-5} mm Hg. One cell with UC was run at 2005°C with a background pressure of 7×10^{-5} mm Hg. The vapor deposited on the stainless steel planchets was analyzed for uranium by fluorometry, and for plutonium [in the case of (UPu)C] it was analyzed by alpha counting. The fuel material, orifice size, exposure times, temperatures, and the weights of the uranium and plutonium found on the planchets are given in Table 5.14.

The mass flow rate was first calculated from these data assuming a constant factor for collection efficiency, 0.0224, determined from a silver standard. The mass effusion rate was then calculated from the mass flow rate using the orifice area at the test temperature, calculated from the area at room temperature, and the thermal expansion coefficient.

The vapor pressure was calculated using the Knudsen equation

$$P_{atm} = C \frac{m}{a} \sqrt{\frac{2\pi RT}{M}}$$

where C = constant = 9.8697×10^{-7} atm-cm^2/dyne

m = mass effusion rate, g/cm^2-sec

a = condensation coefficient

R = gas law constant, ergs/mole-°K

T = absolute temperature, °K.

The small ratio of hole-to-cell areas assured a vapor pressure near equilibrium in the cell.

It was assumed that the (UPu)C evaporates as uranium and plutonium metal vapor in the monatomic state and as carbon vapor in C_1, C_2, and C_3 states. The conden-

TABLE 5.14 — DATA FROM VAPOR PRESSURE RUNS

Experiment	Planchet	Time of Test, min	Temp, °K	Deposited U, μg	Deposited Pu, μg
UC	AB	40	2290	15.0	–
($D_{orifice}$ = 0.0302 in.)	BB	45	2285	32.5	–
	CB	50	2280	50.0	–
	DB	60	2275	67.5	–
	EB	60	2275	–	–
	FB	60	2270	85.0	–
$(U_{0.95}Pu_{0.05})C_{0.98}$	GB	45	2275	13.5	75.0
($D_{orifice}$ = 0.0302 in.)	HB	45	2265	16.0	44.75
	IB	45	2265	17.0	25.1
	JB	45	2270	16.5	18.4
	KB	40	2270	14.5	11.9
	LB	40	2265	14.0	8.70
$(U_{0.95}Pu_{0.05})C_{0.98}$	MB	18	2105	3.0	6.00
($D_{orifice}$ = 0.0413 in.)	NB	21	2100	2.5	7.95
	OB	23	2095	3.0	5.75
	PB	25	2095	2.5	7.70
	QB	43	2095	–	–
	RB	46	2095	2.5	6.90
	SB	60	2095	2.5	11.30
	TB-ZB	309	2095	6.50	130.8

sation coefficient for the metal vapor was taken as unity as it is for most metals. The molecular weight used in the Knudsen equation was also that of atomic uranium and plutonium. A small error is introduced if the actual species is a carbide, but the evidence to date by other investigators indicates a dissociation to metal and carbon. Using the above assumptions, the vapor pressure of uranium and plutonium were calculated. These values, together with the mass effusion rates, are given in Table 5.15.

The original samples and the residues in the cells were analyzed for both plutonium and carbon when sample size permitted. The results are given in Table 5.16. The residues from all three cells were in the form of sintered disks which were crushed before analysis. No interactions were evident between the disks and the tantalum carbide layer.

Early in the program, it was hoped that X-ray diffraction patterns could be obtained from deposits on aluminum planchets. However, previous results with (UPu)C on $(U_{0.8}Pu_{0.2})C$ were disappointing in that the carbide oxidized on the planchet in the time delay between deposition and analysis. Therefore, X-ray diffraction analyses were not made on this program.

5.7.4 Discussion of Results

A. UC Standard

The vapor pressure of arc cast uranium carbide was determined at 2005°C using a cell with an internal tantalum carbide layer of 0.003 in. It is evident that a non-equilibrium condition existed. The value of 2×10^{-6} atm was obtained by extrapolating the data back to zero time. The increasing vapor pressure of uranium over UC means that the sample composition changed with time, probably due to diffusion of carbon across the TaC layer to the Ta of the cell.

TABLE 5.15 — CALCULATED VAPOR PRESSURE DATA

Material	Planchet	Temperature, °K	Mass Effusion Rate, g/cm²-sec × 10⁵		Vapor Pressure, atm × 10⁶	
			U	Pu	U	Pu
UC	AB	2290	5.83	–	4.08	–
	BB	2285	11.3	–	7.90	–
	CB	2280	15.6	–	10.9	–
	DB	2275	17.5	–	12.2	–
	EB	2275	–	–	–	–
	FB	2270	22.1	–	15.4	–
$(U_{0.95}Pu_{0.05})C_{0.98}$	GB	2275	4.67	26.0	3.25	18.1
	HB	2265	5.56	15.5	3.88	10.8
	IB	2265	5.89	8.70	4.11	6.05
	JB	2270	5.74	6.37	4.00	4.43
	KB	2270	5.67	4.63	3.95	3.22
	LB	2265	5.46	3.39	3.81	2.36
$(U_{0.95}Pu_{0.05})C_{0.98}$	MB	2105	1.3	2.81	0.83	1.87
	NB	2100	0.87	3.18	0.58	2.12
	OB	2095	1.0	2.09	0.67	1.40
	PB	2095	0.73	2.59	0.49	1.73
	QB	2095	–	–	–	–
	RB	2095	0.41	1.26	0.27	0.84
	SB	2095	0.31	1.58	0.21	1.05
Combination of seven planchets	TB-ZB	2095	0.156	3.56	0.104	2.38

TABLE 5.16 — ANALYSES OF FUEL MATERIALS FROM
FROM THE DIFFUSION CELLS

Material	Average Temp, °K	Carbon Content, w/o		Plutonium Content, w/o	
		Before	After	Before	After
UC	2280	4.73	4.70	–	–
$(U_{0.95}Pu_{0.05})C_{0.98}$	2270	4.56	*	4.9	0.51
$(U_{0.95}Pu_{0.05})C_{0.98}$	2095	4.56	4.47	4.9	2.31

*Not enough sample available.

B. $(U_{0.95}Pu_{0.05})C_{0.98}$ at 1995°C

The cell used for the 1995°C test with (UPu)C had both an internal and external carbide layer of 0.003 to 0.004 in. The vapor pressure data from Table 5.15 are plotted in Fig. 5.25. The uranium data are fairly constant indicating that nearly equilibrium conditions exist. The zero time extrapolation gave a vapor pressure of U over (UPu)C of 2.7×10^{-6} atm. However, had the cell been run longer, the curve would probably asymptote to the true vapor pressure value, which should be somewhat lower than the value for UC.

The data for plutonium vapor pressure over the (UPu)C show a considerable exponential decrease with time.

The composition data, given in Table 5.16, show that the plutonium content decreased by almost a factor of 10. If nearly equilibrium conditions exist, the concentration (mole fraction) of plutonium in the cell will decrease with time, but the ratio of plutonium partial pressure to plutonium mole fraction should remain constant. The constant is the vapor pressure of pure plutonium over PuC as per Raoult's law. This value can be obtained for zero time and for the total test time (260 min) by plotting the data in another form. Since the original plot was exponential in shape, the equation fitting the data should have the following form:

$$P_t = P_0 e^{-\text{constant} \times \text{time}}$$

Therefore, the log of vapor pressure was plotted vs time. The resulting curve is shown in Fig. 5.26. If the early nonequilibrium points are neglected, the remainder yields a straight line which can be extrapolated to zero time.

Time, min	Plutonium, mole fraction	Vapor Pressure, atm Pu over (UPu)C	Calculated Vapor Pressure, atm Pu over PuC
0	0.049	15×10^{-6}	3.0×10^{-4}
260	0.0051	2.0×10^{-6}	3.9×10^{-4}

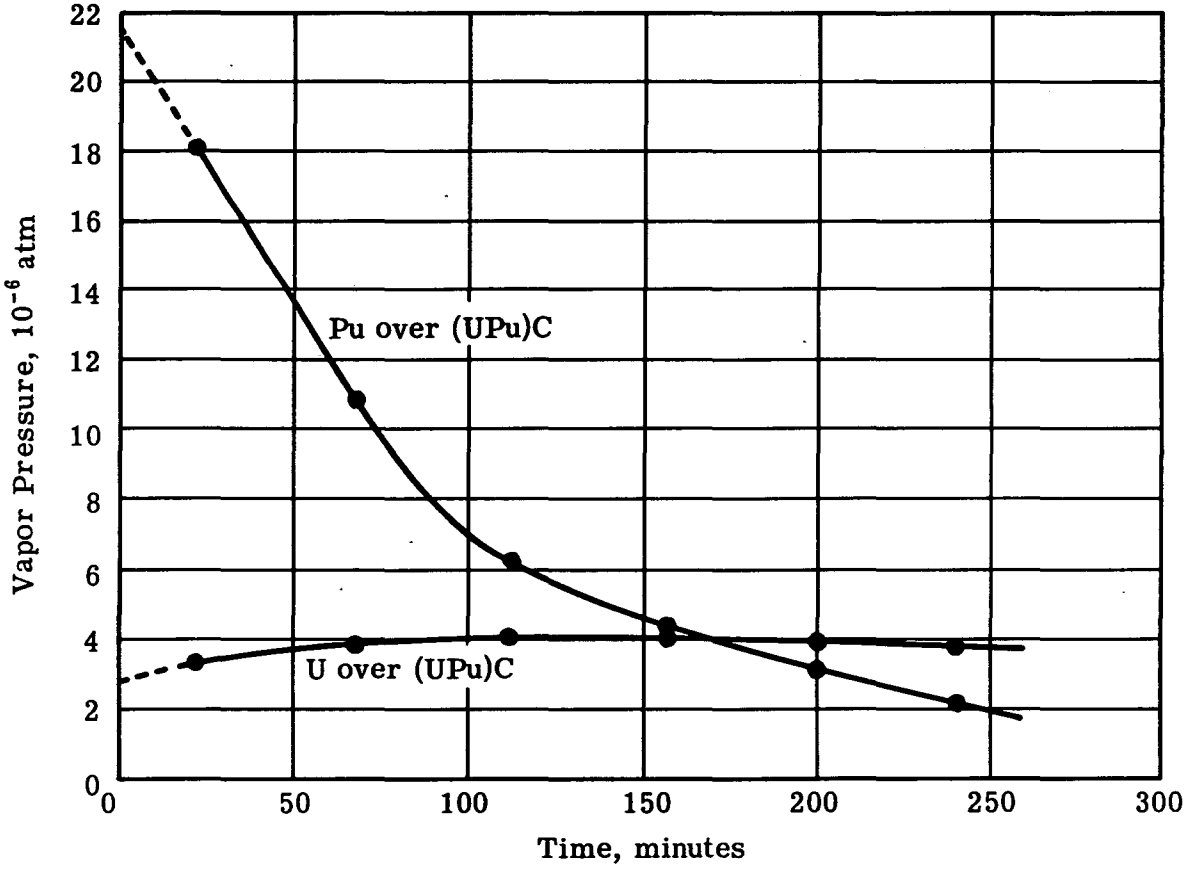

Fig. 5.25 — Vapor Pressure of U and Pu over (UPu)C at 1995°C

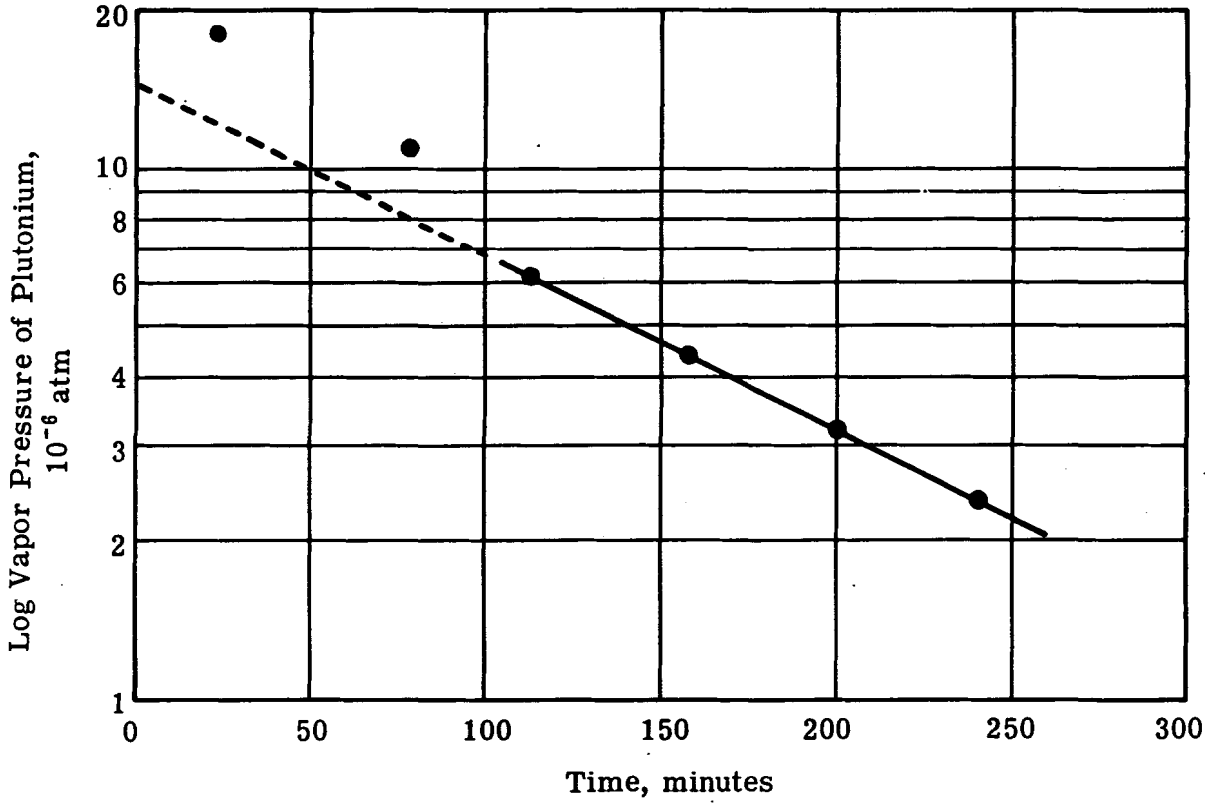

Fig. 5.26 — Log of Vapor Pressure of Pu over (UPu)C at 1995°C

Since the calculated vapor pressures of pure Pu over PuC at zero time and after 260 minutes are in fair agreement, it is likely that the vapor pressure of Pu over $(U_{0.95}Pu_{0.05})C_{0.98}$ is close to 1.5×10^{-5} atm.

$(U_{0.95}Pu_{0.05})C_{0.98}$ at 1822°C

One long test was performed with (UPu)C at 1822°C in a tantalum cell with internal and external carbide layers each thicker than 0.004 in. The cell was carburized essentially through its 0.010-in. wall. The data are plotted in Fig. 5.27. The deposits on the planchets at this lower temperature were so small that they approached the ultimate sensitivity of the chemical analysis method. Therefore, the solutions of the deposits on the last seven planchets were combined and treated as one sample. The data for uranium were in agreement with the first part of the run and the vapor pressure of uranium over (UPu)C approached 9×10^{-8} atm.

The value of the vapor pressure of plutonium over (UPu)C from the combined set was not in agreement with the data from the first part of the run. In addition, the plutonium content of the sample residue in the cell was about half of the starting content. At this time, the vapor pressure of plutonium over (UPu)C can only be estimated to be in the range of 1 to 2×10^{-6} atm. The vapor pressure of plutonium over pure PuC is then estimated to be 2 to 4×10^{-5} atm at 1822°C.

5.8 FUEL REPROCESSING

The major problem in reprocessing uranium carbide-plutonium carbide fuels by liquid-liquid extraction methods is expected to be dissolution of the spent fuel. While UC and (UPu)C dissolve readily in conventional solvents such as nitric acid, the behavior of the irradiated fuel containing fission products is difficult to predict. Laboratory studies on the dissolution of pellets of UC and (UPu)C with selected simulated fission products were made early in the program to provide guidance for the problems of dissolution of the irradiated fuel.

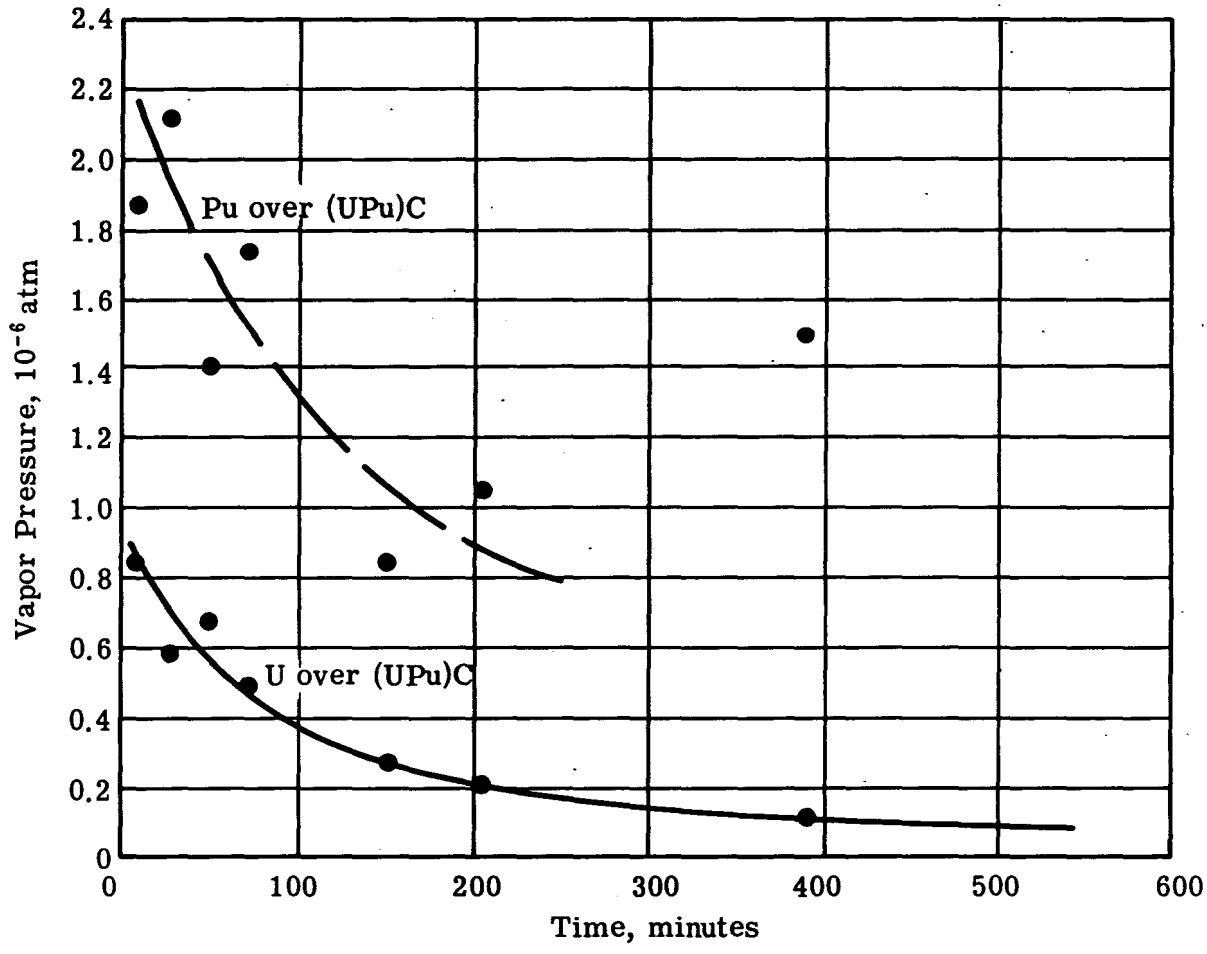

Fig. 5.27 — Vapor Pressure of U and Pu over (UPu)C at 1822°C

UC pellets were made up containing simulated fission products to find out whether they affect the solubility of the pure UC.

The simulated fission products were limited to relatively stable carbide formers. The amounts expected after 70,000 Mwd/T were calculated to be as follows:

Constituent	w/o	Constituent	w/o	Constituent	w/o
UC	96.28	NbC	0.02	ZrC	0.64
LaC_2	0.25	CeC_2	0.58	MoC	0.72
YC_2	0.06	Pd+C	0.61	RuC	0.84

All the elements were added to UC powder as carbide, with the exception of Pd metal powder and a stoichiometric amount of carbon. The carbides were mixed by milling together for 4 hr in a rubber-lined mill with stainless steel balls. Green pellets were pressed at 40,000 psi using Carbowax 6000 as a temporary binder. The pellets were sintered in a vacuum furnace at 1800°C for 1 hr resulting in a bulk density of about 8 g/cm^3.

The pellets were crushed to -100 mesh and treated at 100°C for an hour in various acids; the acids were filtered, and the insolubles were analyzed for uranium:

	8N-HNO_3	HF-HNO_3	HCl-HNO_3
Total Residue, w/o (3.72% of Total Simulated Fission Product Added)	4.24	2.10	7.55
Uranium in Pellet, Left in Residue, w/o	1.2	0.03	Major

The HF-HNO_3 treatment appeared to be the most effective for recovering uranium from "fisside" and indicated that reprocessing problems were not immediately apparent.

In 1960 the responsibility for the reprocessing studies was shifted to Oak Ridge National Laboratory and this project supplied unirradiated and irradiated (UPu)C

for reprocessing at ORNL. Their results are reported in Reference 28. In summary, three head end processes for recovering uranium and plutonium were investigated. The highest burnup (UPu)C reprocessed was the material from capsules UNC-61 and -64, a nominal level of 20,000 Mwd/T. The most successful process was the pyrohydrolysis of the fuel with steam at 750°C to produce virtually carbon free UO_2. The UO_2 in turn was dissolved in nitric acid to produce a Purex solvent extraction feed. Recovery was made of 99.98% of the uranium and 99.93% of the plutonium. Decontamination from fission product gamma activity was a factor of 10^4.

A second process was the direct dissolution of the carbide in 60% HNO_3. The disadvantage of this process is that half the carbide carbon remains in solution in the form of organic compounds that are formed. The organic compounds then have to be degraded by long-time boiling in a strong oxidant. The irradiated (UPu)C was reprocessed successfully by extended refluxing of the fuel solution in strong nitric acid and treatment with permanganate. Since a completely effective method of eliminating the organic acid impurities still remains to be developed, pyrohydrolysis is a preferred reprocessing method.

The low temperature hydrolysis process developed with unirradiated fuel proved to be unsuccessful with irradiated fuel because irradiation passivates the fuel against hydrolysis in water at 80 to 100°C.

6. REFERENCES AND BIBLIOGRAPHY

Reports Published under This Contract

1. Carbide Fuel Development – Phase I Report, NDA 2140-2 (Oct. 1959).
2. Carbide Fuel Development – Phase II Report, NDA 2145-6 (Nov. 1960). (Progress reports during this period: NDA 2145-1, NDA 2145-4, NDA 2145-5).
3. Carbide Fuel Development – Phase III Report, NDA 2162-5 (Sept. 1961). (Progress reports during this period: NDA 2162-1, NDA 2162-3).
4. Carbide Fuel Development – Phase IV Report, UNC-5055 (Mar. 1963). (Progress reports during this period: UNC-5003, UNC-5013, UNC-5030).
5. Carbide Fuel Development – Phase V Report, UNC-5081 (June 1964). (Progress reports during this period: UNC-5056, UNC-5068).
6. Carbide Fuel Development – Progress Report, UNC-5094 (Sept. 1964).

Publications Resulting from This Contract and Associated Work

7. Sofer, G. and Sapir, J.: Potential of Carbide Fuels in Fast Breeder Reactors, Trans. Am. Nucl. Soc., 3:1 (June 1960).
8. Stahl, D. and Strasser, A.: Properties of Solid Solution Uranium-Plutonium Carbides, "Carbides in Nuclear Energy," Vol. 1, Macmillan Co., London, 1964.
9. Taylor, K., McMurtry, C., and Andersen, J.: Sintering Characteristics of UC and (UPu)C With and Without Small Additions of Nickel, "Carbides in Nuclear Energy," Vol. 2, Macmillan Co., London, 1964.
10. Strasser, A., Cihi, J., Sheridan, W., and Storhok, V.: Irradiation Behavior of Solid Solution Uranium-Plutonium Monocarbides, Compounds of Interest in Nuclear Reactor Technology, "Nuclear Metallurgy," Vol. X, Am. Inst. Mech. Eng. (1964).

11. Strasser, A., Cihi, J., Hurwitz, S., and Martin, R.: Irradiation Behavior of Solid Solution Uranium-Plutonium Monocarbides at High Burnups, Third International Conference on Plutonium, London (Nov. 1965). To be published.

12. AEC Uranium Carbide Meetings

Strasser, A.: Carbide Fuel Development at NDA
Taylor, K.: Experimental Work on Uranium Carbide at the Carborundum Company
– from Progress in Carbide Fuels, TID-7589 (Mar. 1960).

Strasser, A.: Carbide Fuel Development at NDA
Taylor, K.: Status of Carbide Fuel Development at the Carborundum Company
– from Proceedings of the Uranium Carbide Meeting Held at ORNL, TID-7603 (Dec. 1960).

Stahl, D. and Strasser, A.: Carbide Fuel Development at the United Nuclear Corporation
Taylor, K., McMurtry, C., and Andersen, J.: Carbide Fuel Development at the Carborundum Company
Bowman, M.: Studies within the System UC-UC_2
– from The Fourth Uranium Carbide Conference, TID-7676 (May 1963).

13. Strasser, A.: Plutonium Fuel Programs of the United Nuclear Corporation, from Plutonium as a Power Reactor Fuel, Am. Nucl. Soc. Topical Meeting, HW-75007 (Dec. 1962).

14. Strasser, A.: Status of the Uranium-Plutonium Carbide Fuel Development Program, from Proceedings of the Conference on Breeding, Economics, and Safety in Large Fast Power Reactors, ANL-6792 (Dec. 1963).

15. Strasser, A., Wheelock, C., and Neimark, A.: Uranium-Plutonium Carbide Fuels for Fast Breeder Reactors, Am. Nucl. Soc. Topical Meeting on Fast Reactor Technology, ANS-100 (Apr. 1965).

Other References

16. Runnalls, O. J. C.: UO_2-Fabrication and Properties, Nucleonics, 17(5):110 (May 1959).

17. Bates, J. L. and Roake, W. E.: Irradiation of Fuel Elements Containing UO_2 Powder, Preprint V-90 of paper presented at the Nuclear Engineering and Science Conference, April 1959.

18. Enrico Fermi Atomic Power Plant, APDA-124 (Jan. 1959).

19. "Directory of Nuclear Reactors," Vol. I, Power Reactor, International Atomic Energy Agency (1959).

20. Survey of Initial Fuel Costs of Large U. S. Nuclear Power Stations, Edison Electric Institute, EEI-59-150 (Dec. 1958).

21. Amorosi, A. and Yevick, J. G.: An Appraisal of the Enrico Fermi Reactor, A/Conf. 15/P/2427, Second International Conference on the Peaceful Uses of Atomic Energy, June 1958.

22. Stahl, D., Strasser, A., Taylor, K., and Andersen, J.: Out-of-Pile Properties of Mixed Uranium Plutonium Carbides, UNC-5074 (Dec. 1963).

23. Taylor, K. and McMurtry, C.: Synthesis and Fabrication of Refractory Uranium Compounds, Summary Report, ORO-400 (Feb. 1961).

24. Crane, J. and Gordon, E.: The Development of Uranium Carbide as a Nuclear Fuel, UNC-5080 (Feb. 1964).

25. Rough, F. and Chubb, W.: Progress on the Development of Uranium Carbide-Type Fuel Materials, Final Report on AEC Fuel Cycle Program, BMI-1554 (Nov. 1961).

26. Ogard, A., Land, C., and Leary, J.: The Thermal Expansion of PuC and PuC-UC Solid Solution, LA-2768 (Oct. 1962).

27. Russell, L. et al.: Monocarbides as Reactor Fuels, P/154, Third Geneva Conference, 1964.

28. Flanary, J. et al.: Hot Cell Studies of Aqueous Dissolution Processes for Irradiated Carbide Reactor Fuels, ORNL-3660 (Sept. 1964).

29. Leary, J. et al.: Thermal Conductivity and Electrical Resistivity of UC, (UPu)C, and PuC, "Carbides in Nuclear Energy," Vol. 1, Macmillan Co., London, 1964.

30. Frost, B., Mardon, P., and Russell, L.: Research on the Fabrication Properties and Irradiation Behavior of Plutonium Fuels for the UK Reactor Programme, Plutonium as a Power Reactor Fuel, Am. Nucl. Soc. Topical Meeting, HW-75007 (Dec. 1962).

31. Rutland, L.: United Nuclear Corp., Personal Communication (Jan. 1962).

32. Taraba, F. and Paine, S.: The Radial Distribution of Thermal Neutron Flux in Cylindrical Fuel Specimens During Neutron Irradiation, ANL-5872 (Aug. 1959).

DISTRIBUTION

	No. of Copies
United States Atomic Energy Commission Division of Reactor Development Washington, D. C.	
Attn: Chief, Liquid Metal Cooled Reactors Branch	3
Chief, Fuels and Development Branch	3
Mr. William Rice	2
Mr. George Packer	2
Mr. Rudolph Grube	1
United States Atomic Energy Commission New York Operations Office New York, New York	
Attn: Mr. J. Wise, Reactor Development Division	3
Reports Librarian	1
United States Atomic Energy Commission New York Patents Group Upton, Long Island, New York	1
Division of Technical Information Extension Oak Ridge, Tennessee	24
United States Atomic Energy Commission Chicago Operations Office Argonne, Illinois	
Attn: Director, Reactor Engineering Division	1
United States Atomic Energy Commission Hanford Operations Office Richland, Washington	
Attn: Mr. John Musser	1

Dow Chemical Company, Rocky Flats,
Boulder, Colorado
Attn: Mr. J. Willging 1

Power Reactor Development Company
Detroit, Michigan
Attn: Mr. R. W. Hartwell 1

General Atomics Division
General Dynamics Corporation
San Diego, California
Attn: P/245 1

Westinghouse Electric Corporation
Atomic Fuel Department
Cheswich, Pennsylvania 1

Atomic Power Development Associates, Inc.
Detroit 26, Michigan 1

Dr. John C. Woodhouse
1 Guest Lane
Wilmington, Delaware 1

Argonne National Laboratory,
Argonne, Illinois
Attn: Mr. R. E. Macherey 1

Combustion Engineering
Windsor, Connecticut 1

Allis-Chalmers Manufacturing Company
Atomic Energy Division
Bethesda, Maryland 1

Westinghouse Electric Corporation
Atomic Power Division
Pittsburgh, Pennsylvania 1